Tetrahedron 65 (2009) 10842–10855

Contents lists available at ScienceDirect

Tetrahedron

journal homepage: www.elsevier.com/locate/tet

A comprehensive picture of the one-electron oxidation chemistry of enols, enolates and α-carbonyl radicals: oxidation potentials and characterization of radical intermediates

Michael Schmittel [a,*], Mukul Lal [a], Rupali Lal [a], Maik Röck [b], Anja Langels [c], Zvi Rappoport [d], Ahmad Basheer [d], Jens Schlirf [e], Hans-Jörg Deiseroth [e], Ulrich Flörke [f], Georg Gescheidt [g]

[a] Department of Chemistry, Organische Chemie I, Universität Siegen, Adolf-Reichwein-Str., D-57068 Siegen, Germany
[b] Institut für Organische Chemie und Biochemie, Universität Freiburg, Albertstr. 21, 79104 Freiburg, Germany
[c] Institut für Organische Chemie der Universität Würzburg, Am Hubland, D-97074 Würzburg, Germany
[d] Institute of Chemistry, The Hebrew University, IL-91904 Jerusalem, Israel
[e] Department of Chemistry, Anorganische Chemie I, Universität Siegen, Adolf-Reichwein-Str., D-57068 Siegen, Germany
[f] Department of Chemistry, Anorganische und Analytische Chemie, Universität Paderborn, Warburger Str. 100, D-33098 Paderborn, Germany
[g] Institut für Physikalische und Theoretische Chemie, TU Graz, Technikerstrasse 4/I, A–8010 Graz, Austria

ARTICLE INFO

Article history:
Received 22 June 2009
Received in revised form
21 September 2009
Accepted 9 October 2009
Available online 4 November 2009

ABSTRACT

Oxidation potentials of 40 enols, enolates and some selected α-carbonyl radicals are presented along with their characterization by various techniques as applicable (X-ray, EPR, ENDOR, general TRIPLE, magnetic susceptibility measurements, UV–vis, fast scan cyclic voltammetry, isotope effects). The model compounds comprise representatives of stable simple enols linked to a multitude of substituents (alkyl, alkenyl, alkynyl, aryl, heteroaryl, propargyl alcohols) and of stable simple enols of amides. The results allow to clarify the primary reaction pathway of enol radical cations as a rapid deprotonation and—if warranted by the redox potential and the strength of the oxidant—a follow-up oxidation of the resultant α-carbonyl radical to the α-carbonyl cation. Moreover, the experimental oxidation potentials were linearly correlated with AM1 computed ionization potentials after correction for solvation. The correlation allows a reliable prediction of oxidation potentials of radicals including α-carbonyl radicals. After computing redox potentials of relevant radicals, the possibility of one-electron transfer between enolates and flavin and the involvement of various radicals of ascorbic acid in oxidation processes were assessed.

1. Introduction

Enols, enolates and α-carbonyl radicals constitute derivatives of the carbonyl group, one of the most important functional groups in synthetic organic transformations, but the rich and rewarding facets of their preparative one-electron oxidation chemistry are only surfacing slowly.[1] While the oxidative transformations of enolates leading to intra-[2] and intermolecular[3] C–C bond formation have already reached some importance as demonstrated by the synthesis of hirsutene,[4] acremoauxin A[5a] and palau'amine,[5b] the one-electron oxidation of enols and α-carbonyl radicals has remained largely unexplored.[1,6–9] Despite such shortcomings, α-carbonyl radicals[10] and enol radical cations have been invoked as reactive intermediates in biological processes.[11]

In contrast, the one-electron oxidation of enol derivatives, such as enol ethers,[12] in particular enol silanes,[13] and enol esters,[14] has received much wider coverage, but will not be addressed here.

Theoretical and experimental investigations have established that the thermochemical stability order of keto/enol tautomers can be inverted upon one-electron oxidation in the gas phase[15] or in solution.[8a,e] As a consequence, enols are much more readily oxidized than the tautomeric ketones (E_{ox}(ketone) ≈ E_{ox}(enol)+1.0 V),[8a] allowing for a selective oxidation of the enol present in minute amounts in the tautomeric equilibrium. In a reaction system designed for rapid enolization, e.g. in the presence of acid, the ketone may now be transformed quantitatively via an enol radical cation as intermediate, opening new synthetic perspectives.[7]

One reason why so little is known about the one-electron oxidation chemistry of enols in solution is connected to their facile tautomerization to the thermodynamically more stable keto form. To outmaneuver this problem we chose β,β-dimesitylethenols as kinetically stable enols, some of which had initially been inspected

* Corresponding author. Tel.: +49 271 7404356; fax: +49 271 7403270.
E-mail address: schmittel@chemie.uni-siegen.de (M. Schmittel).

0040-4020/$ – see front matter © 2009 Elsevier Ltd. All rights reserved.
doi:10.1016/j.tet.2009.10.039

by Fuson and Rowland[16] and more recently investigated in depth by Rappoport et al.[17] Importantly, both the enol and keto tautomers of many of these systems can be obtained in tautomerically pure form.

Herein, we wish to present a study on the oxidation of 40 stable enols (Chart 1), some of which have been synthesized for the first time. We will present the characterization of the enols and their radical cations, enolates and α-carbonyl radicals by cyclic voltammetry (CV), EPR/ENDOR, UV-vis and magnetic susceptibility measurements. Along with some results on the preparative one-electron oxidation of enolates this will provide a comprehensive picture of the enol one-electron oxidation chemistry. Some of the CV results have been described in preliminary communications, but will be repeated here to describe the full picture.[6,8a]

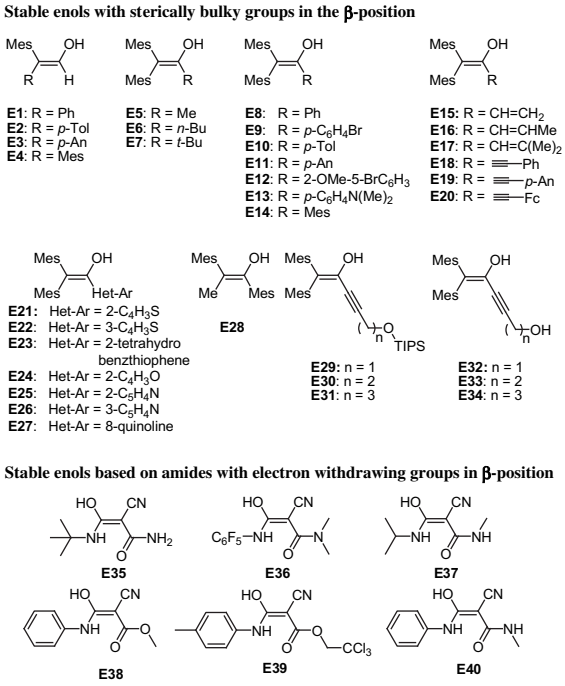

Chart 1. List of enols in the present investigation.

2. Results

2.1. Synthesis and characterization of enols

The synthesis of all enols, except for **E2**, **E3**, **E6**, **E9**, **E12** and **E29**–**E34**, has been described elsewhere.[8b,c,18,19–21] Enols **E2** and **E3** were prepared by following the synthetic protocol to enol **E1** that had initially been reported by Fuson et al.[22] LAH reduction of the corresponding aryl mesityl ketene allowed the isolation of the tautomerically pure (99%) enol **E2** in 17% yield after chromatography. In contrast, enol **E3** could only be prepared in a mixture with the corresponding aldehyde (75% enol). Unfortunately, this enol/aldehyde mixture decomposed quite rapidly presumably due to autoxidation of the readily oxidizable (vide infra) enol tautomer.

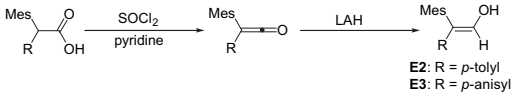

E6, **E9** and **E12** were readily obtained from dimesitylketene and the corresponding alkyl or aryl lithium reagents following procedures developed mainly by Fuson and Rappoport.[16,17b,23]

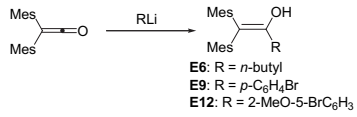

The alkynylated enols **E29**–**E31** were synthesized in reasonable yields (31–80%) by Grignard addition of the corresponding TIPS protected acetylenes to dimesitylketene. The ω-hydroxy enols **E32**–**E34** were obtained in good yields (78–86%) by deprotection of the enols **E29**–**E31** with 10% sulfuric acid in methanol.

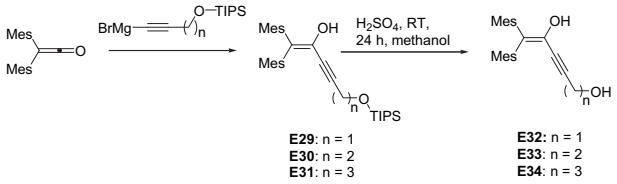

The enols were characterized by IR, ^{1}H NMR, ^{13}C NMR and elemental analysis/HRMS. Suitable single crystals were obtained for **E29** and **E34** and analyzed by X-ray analysis (Fig. 1).

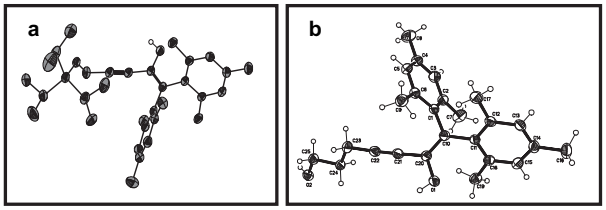

Figure 1. Molecular structure of (a) **E29** and (b) **E34** as obtained by X-ray single crystal analysis. Data are reported in Tables 10 and 11 (see Experimental part).

2.2. Cyclic voltammetric investigations of β,β-dimesityl enols

At low scan rates (v=50–500 mV s^{-1}) CV investigations of all enols displayed two oxidation waves. The first, an irreversible wave was readily assigned to the oxidation of the enol **E** (fourth column in Table 1) and the second wave (mostly partially reversible) to the oxidation of benzofuran derivatives **B** formed rapidly in the course of the enol oxidation (Fig. 2). According to our earlier mechanistic investigations[8a–d] the formation of benzofurans **B** can be understood in terms of the following mechanism (Scheme 1).

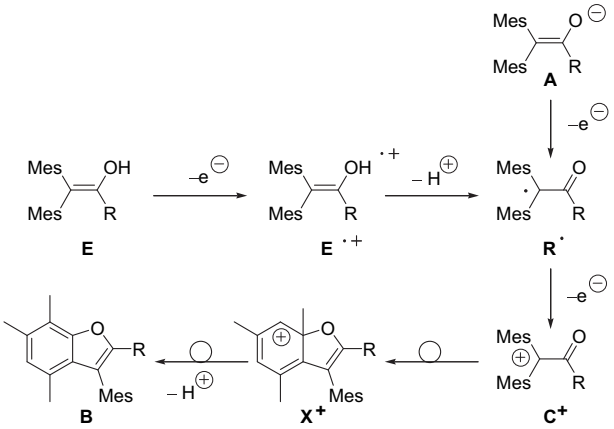

Scheme 1. Mechanism of the oxidation of stable β,β-dimesityl enols **E** or enolates **A**.

Table 1
Oxidation potentials (either E_{pa} or $E^{ox}_{1/2}$ vs ferrocene) of enols and derivatives carrying bulky groups in the β-position. All cyclic voltammograms were recorded in acetonitrile at v=100 mV s^{-1} at room temperature unless noted differently (uncertainty ±10 mV s^{-1})

Model system	$E^{ox}_{1/2}$ of enolates **A**/V_{Fc}	E_{pa} of α-carbonyl radicals **R**$^{\bullet}$/V_{Fc}	E_{pa} of enols **E**/V_{Fc}	$E^{ox}_{1/2}$of enols **E**/V_{Fc}
E1	−0.66[a]	+0.63[a]	+0.70	+0.82[k]
E2	n.d.[b]	n.d.[b]	+0.64	n.d.[b]
E3	n.d.[b]	n.d.[b]	+0.48	n.d.[b]
E4	−0.73[c]	+0.36[c]	+0.68[c]	+0.85[j]
E5	−0.90[c]	+0.21[c]	+0.68[c]	+0.96[j]
E6	−0.87	+0.14	+0.59	n.d.[b]
E7	−1.01[c]	+0.15[c]	+0.64[c]	0.73[n]
E8	−0.83[c]	+0.24[c]	+0.61[c]	+0.67[h,i]
E9	−0.78	+0.29	+0.58	n.d.[b]
E10	−0.86[c]	+0.22[c]	+0.57[c]	+0.64[h,j]
E11	−0.89	+0.31	+0.52	+0.568[h,k], +0.586[l,m]
E12	n.d.[b]	n.d.[b]	+0.61	n.d.[b]
E13	−0.96	+0.09	+0.13	n.d.[b]
E14	−0.75[c]	+0.26[c]	+0.76[c]	+0.76[j]
E15	−0.78	+0.27	+0.69[d]	n.d.[b]
E16	−0.84	+0.23	+0.64[d]	n.d.[b]
E17	−0.92	+0.14	+0.51[d]	n.d.[b]
E18	−0.60	+0.38	+0.72[d]	n.d.[b]
E19	−0.62	+0.31	+0.68[d]	n.d.[b]
E20	−0.66	+0.16	+0.13[e]	n.d.[b]
E21	−0.78[f]	+0.24[f]	+0.53[f]	n.d.[b]
E22	−0.99[f]	n.d.[b]	+0.58[f]	n.d.[b]
E23	−0.77[f]	+0.27[f]	+0.46[f]	n.d.[b]
E24	−0.78[f]	+0.27[f]	+0.50[f]	n.d.[b]
E25	−0.78	+0.11	+0.46,+0.75[g]	n.d.[b]
E26	−0.72	+0.37	+0.36,+0.76[g]	n.d.[b]
E27	−0.56	+0.01	+0.02,+0.53[g]	n.d.[b]
E28	−0.76[l]	+1.38[o]	+0.945	+1.09[l]
E29	−0.61	+0.35	+0.69	n.d.[b]
E30	−0.61	+0.32	+0.67	n.d.[b]
E32	−0.55	+0.34	+0.84	n.d.[b]
E33	−0.56	+0.31	+0.71	n.d.[b]
E34	−0.63	+0.30	+0.74	n.d.[b]

[a] Determined at v=480 V s^{-1}.
[b] Not determined.
[c] From Ref. 6.
[d] From Ref. 18.
[e] Ferrocene residue is oxidized.
[f] From Ref. 20.
[g] From Ref. 19 (low potential=hydrogen bonded species, high potential=no hydrogen bond).
[h] From Ref. 26.
[i] Determined at v=14,000 V s^{-1}.
[j] Determined at v=10,000 V s^{-1}.
[k] Determined at v=12,000 V s^{-1}.
[l] Determined at v=4000 V s^{-1}.
[m] In dichloromethane.
[n] Determined at v=1000 V s^{-1}.
[o] Determined at v=600 V s^{-1}.

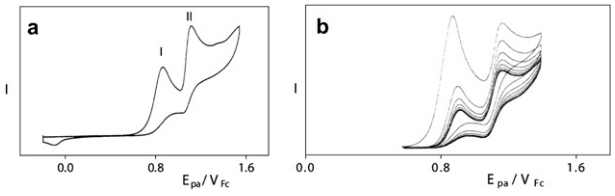

Figure 2. Representative cyclic voltammograms of a β,β-dimesityl enol showing the two typical oxidation waves at 100 mV s^{-1} scan rate; wave I shows the enol oxidation and wave II the oxidation of the benzofuran as a follow-up oxidation product of the enol (in some cases oxidation of dihydrofuranyl cations). (a) CV of **E32** in acetonitrile, (b) multiple scan of **E32**.

The enol oxidation wave exhibited a linear shift of the anodic peak potential with log v and a decreasing ratio $I_{pa}/v^{1/2}$ with increasing scan rate. These diagnostic criteria[24] point to the occurrence of a reversible electron transfer followed by a fast irreversible chemical reaction involving a second electron transfer. Interestingly, in some of the model systems containing strong electron donating groups or five-membered heterocycles, no oxidation wave for the benzofuran was observed. Instead an oxidation wave at higher anodic potentials was observed for these enols, which was due to the oxidation of the dihydrofuranyl cations $\mathbf{X}^{+}$.[25]

2.3. Cyclic voltammetric investigation of enols derived from amides

The use of electron-withdrawing groups in the β-position has been utilized for the first time by Rappoport et al.[19] to generate enols derived from amides. The high enol content (>90%) in non-polar solvents enabled us to investigate their electrochemical properties (Fig. 3, Table 2). All enols **E35**–**E40** exhibited an irreversible oxidation wave between E_{pa}=1.23–1.49 V_{Fc} (except for **E37**, which showed two oxidation waves). An EC_{irr} electrode kinetics was obtained for enols **E35**–**E40** based on the diagnostic criteria by Nicholson and Shain.[24] However, since the HOMO of **E35**–**E40** is dominated by their enamine character, these enols behave differently than the other enols upon oxidation.

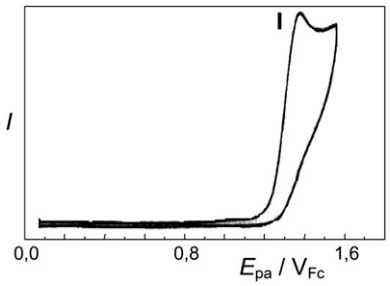

Figure 3. A representative cyclic voltammogram observed for enols derived from amides (i.e. of **E40**) in dichloromethane at a scan rate of 100 mV s^{-1}.

Table 2
Oxidation potentials of enols **E35**–**E40** (derived from amides) in dichloromethane at a scan rate of 100 mV s^{-1}

Enol	E_{pa1}/V_{Fc}	E_{pa2}/V_{Fc}	Shift[a]/V_{Fc}
E35	1.49	—	1.45
E36	1.38		
E37	1.23	1.40	1.19 (E_{pa1}), E_{pa2}-disappears
E38	1.32	—	—
E39	1.38	—	—
E40	1.24	—	—

[a] Shift in the oxidation potential observed upon addition of 2,6-di-*tert*-butylpyridine.

2.4. Characterization of enol radical cations in solution

For some of the enols (**E8**, **E10**, **E11** and **E14**) it was possible to follow the reactivity of their radical cations in acetonitrile using fast scan cyclic voltammetry (FSCV).[26] At scan rates beyond 4000 V s^{-1} their irreversible oxidation waves turned reversible (Fig. 4, Table 3). The different degree of reversibility at various scan rates was utilized for the determination of the rate constants k_f applying the Nicholson–Shain formalism and assuming a rate determining first-order process. The enol radical cation **E11**$^{\bullet+}$ proved to be the one with the longest lifetime both in acetonitrile (τ=6×10^{-5} s) and dichloromethane (τ=1.9×10^{-2} s). A primary kinetic isotope effect KIE=2.6 was found when comparing the follow-up reactions of **E11**$^{\bullet+}$ and [OD]–**E11**$^{\bullet+}$. UV–vis investigations on **E11**$^{\bullet+}$ provided two absorptions, at λ=404 nm and λ=520 nm.

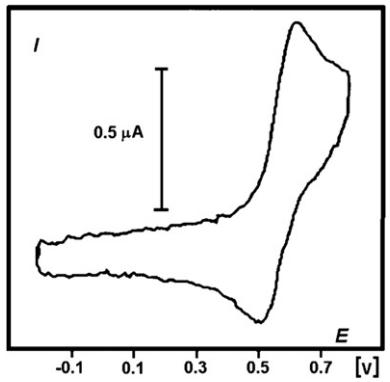

Figure 4. Typical fast scan cyclic voltammogram obtained for a β,β-dimesityl enol: **E11**, scan rate=2000 V s^{-1}, solvent: acetonitrile.

Table 3
Results of fast scan CV investigations with bulky β,β-dimesityl enols in acetonitrile

Compound	v/Vs^{-1}	I_{pc}/I_{pa}	τ/s
E8$^{\bullet+}$	14,000	0.20	6×10^{-5}
E10$^{\bullet+}$	10,000	0.21	8×10^{-5}
E11$^{\bullet+}$	4,000	0.47	6×10^{-5}
E14$^{\bullet+}$	8,000	0.25	4×10^{-4}

Oxidation of **E11** by tris(*p*-bromophenyl)aminium (**TBPA**$^{\bullet+}$) in dichloromethane at −100 °C yielded **E11**$^{\bullet+}$ that exhibited a rather long lifetime. While only an unresolved EPR signal could be observed, it was possible to detect well-resolved ENDOR and general TRIPLE (Fig. 5) spectra providing the isotropic hyperfine coupling constants (hfcs). Moreover, the comparison with the spectra of the corresponding deuterated derivative [OD]–**E11**$^{\bullet+}$ permitted further insight into the electron distribution of **E11**$^{\bullet+}$ (Table 4). The structure of **E11**$^{\bullet+}$ will be discussed below in comparison to that of radicals **R4**$^{\bullet}$–**R14**$^{\bullet}$.

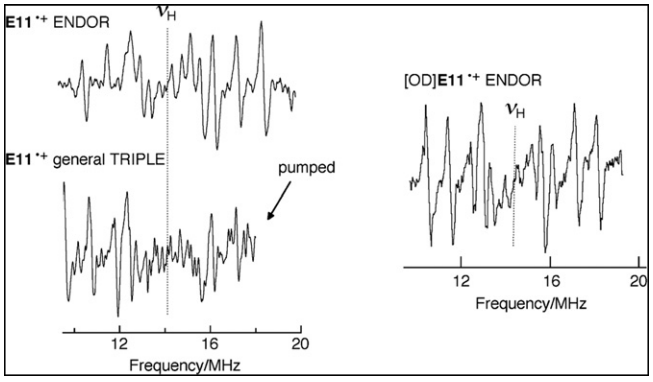

Figure 5. ENDOR spectra of [OH]–**E11**$^{\bullet+}$ and [OD]–**E11**$^{\bullet+}$.

Table 4
Coupling constants (hfc/mT) for **E11**$^{\bullet+}$ and [OD]–**E11**$^{\bullet+}$ obtained by the ENDOR and general TRIPLE spectra in dichloromethane

	Mes(*p*)	Mes(*o*)	Mes(*m*)	An(*o*)	An(*p*)	An(*m*)	O–*H*
E11$^{\bullet+}$	0.307	0.226	0.151	0.109	0.080	—	0.052
[OD]-**E11**$^{\bullet+}$	0.308	0.229	0.150	0.107	0.076	—	–
Calc[a]	0.30	0.15	0.11	0.10	0.08	0.0	0.0

[a] UB3LYP/6–31G**.

2.5. Oxidation of the enolates and characterization of the α-carbonyl radicals

Deprotonation of the enols **E** with 1 equiv of tetramethylammonium hydroxide yielded the corresponding enolates **A**. For all enolates with mesityl groups in the β-position, the cyclic voltammogramms showed a reversible oxidation (Fig. 6). Their half wave oxidation potentials $E^{ox}_{1/2}$ lie between −0.55 and −1.02 V_{Fc} (Table 1). They are much lower than those observed for enolates with β-electron-withdrawing groups.[27]

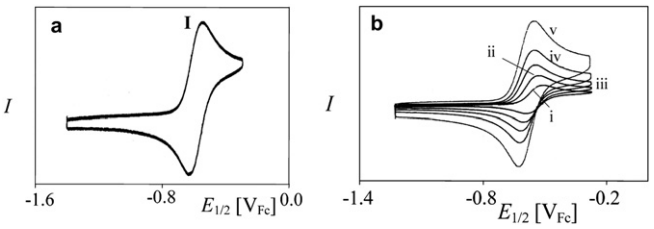

Figure 6. Cyclic voltammograms that show the typical behavior of enolates with bulky β,β-dimesityl groups, (a) completely reversible redox wave of enolate **A12**, (b) scan rate dependence of the oxidation wave of enolate **A12**, (i) 20 mV s^{-1}, (ii) 50 mV s^{-1}, (iii) 100 mV s^{-1}, (iv) 200 mV s^{-1} and (v) 500 mV s^{-1}.

Aside from the reversible oxidation wave of the enolates, an irreversible oxidation wave at higher anodic potential (E_{pa} between +0.01 and +1.38 V_{Fc}) was observed that was assigned to the oxidation of the α-carbonyl radical (Table 1).

For a few selected enolates the formation of the α-carbonyl radicals was furthermore corroborated by EPR/ENDOR and magnetic susceptibility measurements. For EPR/ENDOR experiments the α-carbonyl radicals were generated by one-electron oxidation of enolates **A4**, **A5**, **A7**, **A8**, **A10**, **A11** and **A14** in dichloromethane using 1 equiv of the weak oxidant tri(*p*-anisyl)aminium hexafluorophosphate ($E^{red}_{1/2}$=0.16 V_{Fc}). Upon addition of the oxidant to the enolate a red color emerged immediately. The UV–vis spectrum of **R7**$^{\bullet}$ exhibited two absorptions at λ_1=353 nm and λ_2=480 nm with λ_1 showing a hypsochromic shift of about 17 nm compared to the enolate spectrum. The α-carbonyl radical **R11**$^{\bullet}$ revealed bathochromically shifted absorptions at λ_1=425 nm and λ_2=584 nm.

The structural assignment of the neutral radicals **R4**$^{\bullet}$, **R5**$^{\bullet}$, **R7**$^{\bullet}$, **R8**$^{\bullet}$, **R10**$^{\bullet}$, **R11**$^{\bullet}$ and **R14**$^{\bullet}$ was established by using the hyperfine data obtained by EPR/ENDOR/general TRIPLE. An example is shown in Figure 7 for **R4**$^{\bullet}$; the complete set of hyperfine data is summarized in Table 5. The formation of α-carbonyl radicals in **R7**$^{\bullet}$ and **R11**$^{\bullet}$ was further quantified by magnetic susceptibility measurements using the Evans' NMR shift method,[28] attesting 85±2% (**R7**$^{\bullet}$) and 87±2% (**R11**$^{\bullet}$) conversion to the α-carbonyl radical.

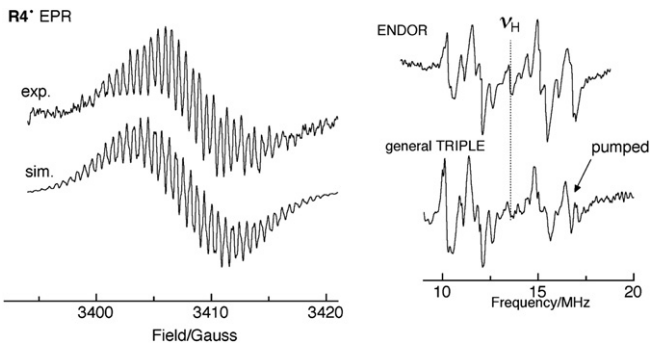

Figure 7. Experimental and simulated EPR, ENDOR and general TRIPLE spectra of α-carbonyl radical **R4**$^{\bullet}$.

Table 5
g-Values of some α-carbonyl radicals at 213–253 K

Compound	*g*-Values	Coupling constants ^{1}H hfc/mT
R4$^{\bullet}$	2.00370	0.234 [a]; 0.181 [b]; 0.136 [b]; 0.106 [c]; 0.069
R5$^{\bullet}$	2.00303	0.221 [a]; 0.177 [b]; 0.149 [b]; 0.116 [c]; 0.096; 0.075
R7$^{\bullet}$	2.00352	0.278 [a]; 0.155 [b]; 0.107 [b]; 0.040 [c]; 0.016
R8$^{\bullet}$	2.00262	0.225 [a]; 0.199 [b]; 0.170 [b]; 0.142 [c]; 0.108; 0.085
R10$^{\bullet}$	2.00339	0.226 [a]; 0.203 [b]; 0.170 [b]; 0.108 [c]; 0.086; 0.010
R11$^{\bullet}$	2.00274	0.227 [a]; 0.203 [b]; 0.170 [b]; 0.111 [c]; 0.087
R14$^{\bullet}$	2.00325	0.194 [a]; 0.165 [b]; 0.132 [b]; 0.106 [c]; 0.085; 0.062; 0.25; 0.14; 0.04
R11$^{\bullet}$	Calcd	0.23 [a]; 0.16 [b]; 0.12 [b]; 0.16 [c]; 0.09

[a] *p*-CH_3–Mes.
[b] *o*-CH_3–Mes (the four *o*-CH_3 groups in the Mes substituents are pairwise equivalent).
[c] *m*-H-Mes. The small hfcs are attributed to protons of the remaining substituents.

2.6. Oxidation of enolate A7 with flavin

Flavin cofactors (FAD and FMN) are known to serve as biological oxidants, e.g. in enzymatic reactions involving dehydrogenations (D-lactate dehydrogenase, general acyl-coenzyme A dehydrogenase, glutaryl-CoA and butyryl-CoA dehydrogenase).[29] Enolates are suggested to be the key intermediates in these oxidations, although the oxidation by flavin cofactors should be very endergonic.[10]

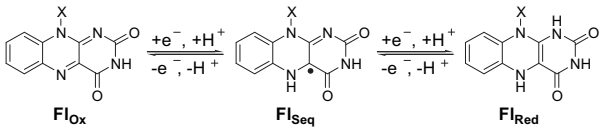

Fl_{Ox} Fl_{Seq} Fl_{Red}

With the oxidation potentials of enolates and α-carbonyl radicals being known through the present work, we planned to mimic the enzymatic oxidation of enolates by $\mathbf{Fl_{Ox}}$ using an endergonic oxidation in solution. Thus, a solution of $\mathbf{Fl_{Ox}}$ ($E_{1/2}$=–0.21 $V_{Ag/AgCl}$[30]) was added to **A7** ($E^{ox}_{1/2}$=–0.83 $V_{Ag/AgCl}$) in equimolar amounts under inert atmosphere. Although electron transfer is endergonic by 620 mV, a deep red coloration was observed after warming the reaction mixture to 50 °C. EPR characterization of the solution indicated the presence of a radical species at *g*=2.0035 with a coupling of 1.5 G and a spectral width of 30.7 G, which was similar to that of the α-carbonyl radical **R7**$^{\bullet}$, generated by oxidation of enolate **A7** with the aminium salt. Addition of sodium bicarbonate to the solution of **A7** and $\mathbf{Fl_{Ox}}$ followed by extraction in DCM afforded the enol **E7** in 74% yield. In contrast, formation of the benzofuran derivative **B7** was not observed.

2.7. Preparative scale oxidation of enols

The benzofuran derivatives **B6**, **B9** and **B12** were isolated after oxidation of the corresponding enols (**E6**, **E9** and **E12**) with 2 equiv of $[Fe(Phen)_3]^{3+}$ (Phen=1,10-phenanthroline) in acetonitrile under inert atmosphere. Compounds **B6**, **B9** and **B12** were obtained in good yields and characterized by ^{1}H NMR, ^{13}C NMR, IR, and HRMS.

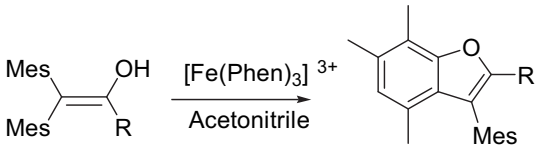

E6 R = *n*-Bu **B6** (86%)
E9 R = *p*-C_6H_4Br **B9** (96%)
E12 R = 2-OMe-5-BrC_6H_3 **B12** (75%)

CV investigations on benzofurans **B6** and **B9** showed partially reversible waves appearing at $E^{ox}_{1/2}$=0.92 and 0.90 V_{Fc}, respectively. The position and form of the wave were identical to that of benzofurans **B** formed during the cyclic voltammetric investigation of enols and enolates.

3. Discussion

3.1. Structural features of the enols

The basic structural features of β,β-dimesityl enols (C=C, C–O bond lengths, etc.) do not alter dramatically upon changes of substituents. Hence, it is not surprising to see that all bond lengths, bond angles and torsional angles in **E29** and **E34** have almost identical values (see Experimental part, Tables 10 and 11). It is noteworthy that the two enols are even similar with regard to the HOC=C torsional angle. Both, **E29** and **E34** prefer an *anticlinal* conformation of the enolic hydroxyl group in the solid state. The latter preference may arise due to OH···π interactions with the unsaturated triple bond. This interaction is dominating over the OH···π interactions with the enol double bond as well as the β-mesityl group, the latter being possible in a *syn* conformation. In addition, the *anticlinal* OH group in **E29** is involved in intermolecular hydrogen bonding in the solid.

3.2. Oxidation potentials of enols

An analysis of the oxidation potentials of enols **E1**–**E34** indicates that a common trend does not exist between the substitution pattern and the oxidation potentials of the enols. However, some interesting features were observed in smaller subgroups. For enols **E8**, **E10**, **E11**, and **E14** a linear relationship was observed between the calculated IP_a and the experimentally determined oxidation potentials (E_{pa}).[19] As anticipated, the calculated IP_a as well as the oxidation potentials decreased with increasing electron-donating ability of the α-aryl ring. Moreover, within a small set of enols, i.e. **E4**, **E5**, **E14** and **E28**, an unusual β-effect of a methyl group was observed. For **E14** (E_{pa}=0.76 V_{Fc}) with three mesityl groups in β,β and α-position, the oxidation potential was found to be higher than when the α-mesityl group was replaced by a hydrogen (**E4**: E_{pa}=0.68 V_{Fc}) or with a methyl group as in **E5** (E_{pa}=0.68 V_{Fc}). Interestingly, enol **E28** (formally the β-mesityl in **E14** is replaced by a methyl group) has an oxidation potential, which is anodically shifted by almost 200 mV (E_{pa}=0.95 V_{Fc}). Comparison of the oxidation potentials of enols **E1**–**E3** reveals that with increasing electron-donating ability of the β-substituent the oxidation potential shifts cathodically by more than 200 mV. Attaching a triple bond in the α-position (**E18**–**E20**, **E29**, **E30**, **E32**–**E34**) has little or no effect on the oxidation potential except for **E20** due to the additional ferrocene substituent. Within the series **E15**–**E17**, a cathodic shift of up to 180 mV was observed (**E15**: E_{pa}=0.69 V_{Fc}, **E16**: E_{pa}=0.64 V_{Fc}, **E17**: E_{pa}=0.51 V_{Fc}) as the number of terminal methyl groups at the α-vinyl group increases.

Unusually low oxidation potentials were observed for all enols with heteroaromatic rings in the α-position. This behavior in enols **E21**–**E25** is due to the enhanced electron density in the enol itself.[20] In contrast, in enols **E26**–**E27** it is primarily due to OH···N hydrogen bonding.[19]

3.3. Radical cation E11$^{\bullet+}$ and neutral radicals—structural considerations

It has been possible to observe enol radical cations in solution by both CV and EPR/ENDOR.[26] For **E11**$^{\bullet+}$, the life times lie in the range between 19 ms (dichloromethane) and 400 μs (acetonitrile) as established by CV. Our investigations nicely complement the laser flash photolysis characterization of the 4-methoxyphenylacetone enol radical cation by Schepp[9] that exhibited a lifetime of 200 μs in acetonitrile. Fortunately, under our experimental conditions, the radical cation **E11**$^{\bullet+}$ was sufficiently long-lived to be characterized by EPR/ENDOR and TRIPLE resonance. Although the multiplicity of the hfcs in **E11**$^{\bullet+}$ could not be directly determined by the analysis of the unresolved EPR signal, structural information was obtained by comparison with the deuterated derivative [OD]-**E11**$^{\bullet+}$ and calculated values. The highest ^{1}H hfc of 0.307 mT was attributed to six equivalent protons of the two *p*-CH_3 groups of the mesityl substituents agreeing rather well with that of the dimesityl methyl radical (0.331 mT).[31] The values 0.226 (6H) and 0.151 (6H) mT were assigned to two sets of *ortho* methyl groups of the mesityl substituents (dimesityl methyl 0.207 mT); due to steric hindrance in **E11**$^{\bullet+}$, two different ^{1}H hfcs were attributed to the two symmetrically non-equivalent *ortho* methyl groups of the mesityl substituents. The ^{1}H hfc of 1.09 mT stems from the *meta* protons. This allotment of the ^{1}H hfcs is compatible with the overall width of the unresolved EPR signal of **E11**$^{\bullet+}$ and reflects a marked 'diaryl methyl' radical character of **E11**$^{\bullet+}$ with the highest spin population residing at C(2). A much smaller spin population in the remainder of the molecules is indicated by comparison with the results on [OD]–**E11**$^{\bullet+}$. While all hfcs remain virtually unchanged, the smallest coupling constant of 0.052 mT vanished indicating that it has to be connected with the proton of the enol OH. These findings corroborated a twisted geometry for **E11**$^{\bullet+}$ along the C(1)–C(2) double bond, which is consistent with results of DFT (UB3LYP/6-31G**) geometry optimizations and the corresponding spin distribution. This also points to a distonic character of **E11**$^{\bullet+}$: whereas the spin resides in the dimesityl methyl radical moiety, the positive charge is predominately located at C(1) and in the anisyl substituent.

The spin distribution in the neutral radicals **R4**$^{\bullet}$, **R5**$^{\bullet}$, **R7**$^{\bullet}$, **R8**$^{\bullet}$, **R10**$^{\bullet}$, **R11**$^{\bullet}$ and **R14**$^{\bullet}$ is similar to that of **E11**$^{\bullet+}$ but with attenuated ^{1}H hfcs in the mesityl substituents. Here, at least partly resolved EPR spectra allowed the determination of the multiplicities of the hfcs. Generally, the spectra are dominated by line patterns, which can be traced back to three sets of ^{1}H hfcs of ca. 0.2–0.25, 0.14–0.19, and ca. 0.1 mT, each due to six equivalent protons. In agreement with the calculations (see Table 6) and related bi(aryl)methyl radicals,[32] the biggest hfcs have to be assigned to two virtually equivalent *para* CH_3 groups of the two mesityl substituents whereas the smaller ones have to stem from two sets of the non-equivalent *ortho*-CH_3 groups. The remaining definitely smaller hfcs are ascribed to the *meta* protons of the mesityl substituent and to further protons of the substituents at C(1), which only carry a minor amount of spin.

Table 6
Selected calculated bond lengths/Å and angles/° for **E11**, **E11**$^{\bullet+}$, and **R11**$^{\bullet}$ (UB3LYP/6-31G**). For numbering, see Scheme 2

	a/Å	*c*/Å	*b*/Å	Out-of plane angle of mesityl substituents/deg	Torsional angle (*b*–*a*–*d*)/deg
E11	1.367	1.375	1.508	57	166
E11$^{\bullet+}$	1.423	1.343	1.480	50	155
R11$^{\bullet}$	1.483	1.238	1.475	48	146

The structural differences between the parent enol, the corresponding radical cation and the neutral radical can be followed by regarding some significant torsion angles and bond lengths of the calculated geometries of **E11**, **E11**$^{\bullet+}$, and **R11**$^{\bullet}$ (Scheme 2, Table 6).

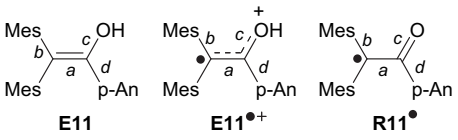

Scheme 2. Compounds **E11**, **E11**$^{\bullet+}$ and **R11**$^{\bullet}$.

The torsional angle between the bonds *b*–*a*–*d* (Scheme 2) is a suitable indicator for the planarity of the molecule in respect to the twist about the central C(1)–C(2) bond. The closer this angle is to 180°, the more planar the molecule. The neutral enol **E11** with a formal conjugated double bond (bond length 1.367 Å) represents a virtually planar system, whereas the radical cation **E11**$^{\bullet+}$ possesses an elongated double bond (1.423 Å) and a more pronounced deviation from planarity (angle *b*–*a*–*d*=155°). Finally, radical **R11**$^{\bullet}$ mirrors a carbon-centered dimesityl radical with an α-carbonyl substituent. In **R11**$^{\bullet}$, the C(1)–C(2) bond length further increases to 1.483 Å and the carbonyl CO bond approaches a double bond (1.238 Å). Remarkably, the out-of-plane angles for the two mesityl substituents are almost identical in **R11**$^{\bullet}$ and **E11**$^{\bullet+}$. Therefore, the lower ^{1}H hfcs for **R11**$^{\bullet}$ compared to **E11**$^{\bullet+}$ can only be rationalized by an increase of the σ character at the radical center C(2) in **R11**$^{\bullet}$ causing attenuated delocalization onto the two mesityl substituents.

Extensive investigations on enols containing electron-withdrawing groups in the β-position (as in **E35**–**E40**) reveal that the follow-up reactions of α-carbonyl radicals derived from these enols are predominantly of the radical type, which is in agreement with previous investigations.[33] In contrast, α-carbonyl radicals derived from β,β-dimesityl enols are kinetically stable due to the bulky groups preventing dimerization. This is clearly demonstrated by the fully reversible enolate oxidation wave in the CV for **E1**–**E34**. With α-carbonyl radicals derived from β,β-dimesityl enols it was thus possible for the first time to measure their oxidation potentials directly by cyclic voltammetry. They agree qualitatively with the reduction potentials of three related α-carbonyl cations determined by Okamoto.[34] All α-carbonyl radicals (Table 1) showed an irreversible oxidation wave under cyclic voltammetric conditions due to fast follow-up reactions of the corresponding carbocations. These reactions furnished the benzofuran derivatives **B** (Scheme 1),[7,8,18,25,35] some of which were isolated and investigated earlier. Partially reversible to irreversible oxidation waves were observed for the benzofuran derivatives.

3.4. Comparison of oxidation potentials of α-carbonyl radicals with other carbon-centered radicals

Due to the kinetic stability of α-carbonyl radicals we were able to directly measure their oxidation potentials[33a] in solution, whereas in general the determination of oxidation potentials of simple carbon-centered radicals requires complicated experimental set-ups. A while ago, Wayner et al.[36] developed a technique to measure oxidation and reduction potentials of carbon-centered radicals but published data on a series, which did not include α-carbonyl radicals. With the knowledge of oxidation potentials of various carbon-centered radicals[36] and our values at hand we were interested to establish a correlation between measured oxidation

potentials in solution and gas phase ionization potentials. When we calculated the gas phase ionization potentials of the carbon-centered radicals described by Wayner et al.[36] using a time inexpensive method (AM1, Spartan programme) and plotted them against the oxidation potentials measured in solution, a linear plot with a rather poor correlation coefficient of R^2=0.88 was obtained.

However, when the gas phase ionization potentials were corrected for the solvation term ΔE_{solv}^{ACN} (Eq. 1) using the Born equation, an improved correlation R^2=0.92 was found between the IP_a^{corr} versus the measured oxidation potential (Eq. 2). The corrected ionization potentials were about 1.6–2.4 eV lower than the gas phase ionization potentials.

$$IP_a^{Corr} = IP_a^{gas} - \Delta E_{solv}^{ACN} \quad (1)$$

$$IP_a^{Corr} = 0.93E_{pa} + 5.48 \quad (2)$$

The validity of Eq. 2 was checked by predicting the oxidation potentials of α-carbonyl radicals **41**•–**44**•, whose oxidation potentials had been measured indirectly by Le-Moing by the reduction of stable carbocations.[37] Importantly, the calculated oxidation potentials using Eq. 2 were in close agreement with the experimentally determined values (Table 7).

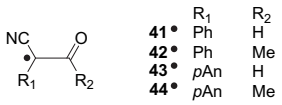

	R_1	R_2
41•	Ph	H
42•	Ph	Me
43•	*p*An	H
44•	*p*An	Me

Table 7
Comparison of calculated and experimental solution oxidation potentials of α-carbonyl radicals.[37] The computed values were obtained by Eq. 2. The solvation term was obtained using the classical Born equation

System	IP_a^{gas} /eV	ΔE_{Solv}^{ACN}/eV	$IP_a^{gas}-\Delta E_{solv}^{ACN}$/eV	Calculated $E_{1/2}/V_{SCE}$	Experimental $E_{1/2}/V_{SCE}$[37]
41•	8.80	1.87	6.93	1.56	1.52
42•	8.56	1.77	6.79	1.41	1.48
43•	8.30	1.72	6.58	1.18	1.19
44•	8.09	1.64	6.45	1.04	1.15

Thus, Eq. 2 can be used for predicting the oxidation potentials of other carbon-centered radicals. However, from the data in Table 7 it is also clear that deviations between 10 and 110 mV may exist between calculated and experimentally determined oxidation potentials. To improve the correlation, we finally combined the α-carbonyl radicals reported by Orliac-Le-Moing et al.,[37] some representative α-carbonyl radicals from Table 1 and Wayner's data. Again, it was necessary to include a solvent correction (Eq. 3, R^2=0.94) providing only a slight change in the overall equation (Fig. 8).

$$IP_a^{Corr} = 0.93E_{pa} + 5.50 \quad (3)$$

Interestingly, in the plot of Figure 8 the oxidation potentials of α-carbonyl radicals derived from β,β-dimesityl enols fall in the same range as benzyl radicals (simple as well as benzannulated ones).

3.5. Biological relevance of oxidation potentials of enols, enolates and α-carbonyl radicals

The enol forms of simple carbonyl compounds are present at exceedingly low concentration in solution ($K_{enol}=10^{-8}$), however,

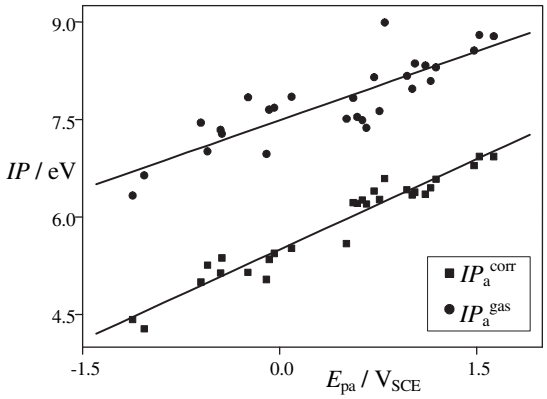

Figure 8. Plot of *IP* (eV) against E_{pa} (V_{SCE}) of carbon-centered radicals including the α-carbonyl radicals derived from β,β-dimesityl enolates. Dots [●] represent a plot of IP_a^{gas} against E_{pa} while dots [■] depict the plot of IP_a^{corr} (IP_a^{gas} corrected for solvation term) against E_{pa} (V_{SCE}).

their concentrations in biological systems may approach unity or even favor enol formation. Enols have been invoked in a number of reactions carried out by racemases.[38] Typically, under biochemical conditions rapid equilibration of the keto/enol/enolate system[39] and its breakdown may occur by one of the following three ways: (a) reversible reaction with an electrophile leading to bond formation/cleavage α to the carbonyl groups[40] (e.g. decarboxylation[41]), (b) eliminations leading to α,β-unsaturated carbonyl compounds,[42] (c) oxidations leading to loss of one or two electrons.[43]

Although involvement of enols as one-electron transfer donors in biological systems is not yet widely established, radical cations of simple enols and enol ethers are known to play a vital role in DNA damage.[44] In addition, enol radical cations have been invoked in transformations carried out by coenzyme B_{12} dependent enzymes such as ribonucleotide reductase, diol and glycerol dehydratase and ethanol-amine ammonia lyase.[45]

The oxidation potentials of our model enols (with or without electron-withdrawing group in the β-position) strongly suggest that a biological oxidation would not occur directly from the enol form (oxidation potentials of simple enols would be much higher than those of β,β-dimesityl enols), but may occur from the corresponding enolates, which are more than 1.5 V (~35 kcal mol^{-1}) easier to oxidize. Also model studies suggest that hydrogen bonding to enols may shift the oxidation potentials of enols by up to 500 mV.[19] Generation of an enolate not only generates a better electron donor, it also allows the system to act as either one- or two-electron transfer reagent, with the second transfer involving the α-carbonyl radical as reducing agent.

Formation of **R7**•, as described in Section 2.6, is in line with electron transfer between $\mathbf{Fl_{Ox}}$ and enolate **A7**. The lack of benzofuran formation clearly indicates that further oxidation of the α-carbonyl radical by $\mathbf{Fl_{Seq}}$ or $\mathbf{Fl_{Ox}}$ did not occur in solution. Radical addition reactions between the $\mathbf{Fl_{Seq}}$ and various simple radicals are well known, but such a process can be excluded for the sterically crowded **R7**•. Thus, after one-electron transfer the reaction stops. Interestingly, investigations by Armstrong and Rizwan[46] indicated that the α-carbonyl radical obtained by dehydration of ethylene glycol radical did neither add to the $\mathbf{Fl_{Seq}}$ nor undergo further oxidation, which is in agreement with the above result.

Obviously, the oxidation of enolates by an enzyme might proceed in an entirely different manner, as conformational changes in the protein or hydrogen bonding to the semiquinone $\mathbf{Fl_{Seq}}$ can potentially bring about a distinct anodic shift in the oxidation potential, allowing for a second electron transfer from the substrate to yield $\mathbf{Fl_{Red}}$. Nevertheless, as the protonated semiquinone form of the riboflavin ($\mathbf{Fl_{Seq}}$) was unable to oxidize the electron rich

α-carbonyl radical **R7•**, which upon oxidation undergoes a fast follow-up reaction, the one-electron oxidation of an α-carbonyl radical derived from a thioester (simplified model for the enzyme substrate) can now be assessed realistically. The oxidation potential of the α-carbonyl radical **45** derived from methyl thioacetate, used here as a simple mimic for the enzyme substrate of a dehydrogenase, is predicted to be 1.92 V_{SCE} (from Eq. 3). This value is clearly far out of range, so that oxidation of **45** by $\mathbf{Fl_{Seq}}$ or $\mathbf{Fl_{Ox}}$ is impossible. The results thus show that flavins may trigger a one-electron oxidation of enolates, but they do not have the oxidation power to oxidize α-carbonyl radicals.

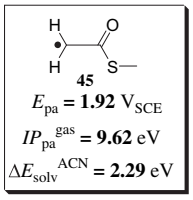

The data of this manuscript also allow to get better insight into the action of vitamin C. Ascorbic acid (vitamin C), an important two-electron donor system, has found a broad range of applications in various fields ranging from photographic developing agents,[47] metal ion sensors to its famous utility as a biological antioxidant. While the electron donating ability of ascorbic acid is well accepted, the mechanism by which it donates the electron is, however, still not well understood, mostly due to the multitude of possible reductants (Scheme 3).

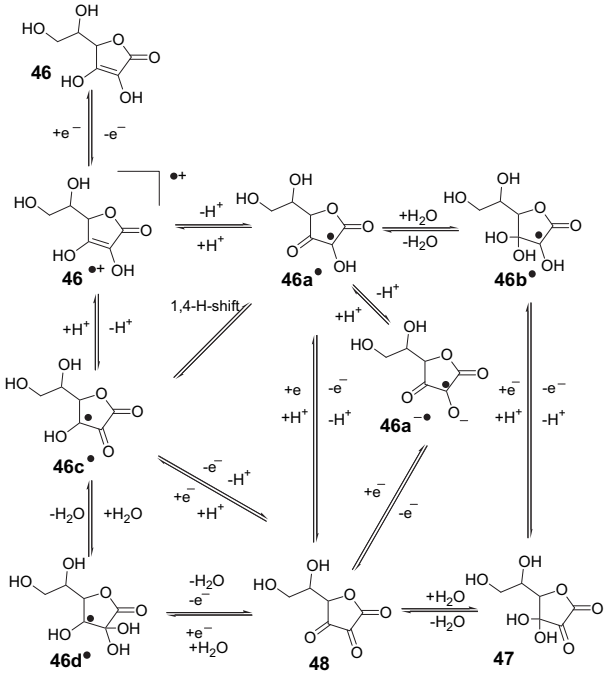

Scheme 3. The various possible radicals that are formed after one-electron oxidation of ascorbic acid (**46**).

The radical anionic ascorbate **46a**$^{-\bullet}$ has been invoked as an important intermediate after one-electron transfer,[48] as support was gained by a mechanistic investigation based on two-dimensional voltammetry.[49] The half wave potentials were found to be strongly pH dependent (0.76 V_{SCE} at pH 2.1 and 0.3 V_{SCE} at pH 6.7,[49] 1.13 V_{SCE} in DMF[50]).

Recent theoretical calculations revealed that approximately 40% of the unpaired spin resided on the O2 position in the ascorbic acid radical **46a•**.[51] It was also predicted that hydrogen bonding occurring at O2 and O3 atoms would lead to a significant redistribution of spin density in the free radical **46a•**. Interestingly, due to an absorption at 290 nm, the presence of **46c•** was established under pulse radiolytic conditions. The spectrum was shifted hypsochromically by 70 nm in comparison to **46a•**.[52] Earlier pulse radiolytic investigations in nitrous oxide saturated solution between pH 3.0 and 4.5 showed two OH–radical adducts (**46b•** and **46d•**) in addition to the ascorbate radical anion.[53] The OH–radical adduct **46b•** formed by addition of the hydroxyl radical to C3 of **46**. Radical **46b•** was found to exhibit a doublet of lines in the EPR that is pH dependent. Equally, the adduct **46d•** could form by addition of the hydroxyl radical to the C2 position of **46**. It is apparent from Scheme 3 that a large number of potential secondary electron donors can be written for ascorbic acid radical, some of which have the structure of α-carbonyl radicals or α,α′-dicarbonyl radicals. It would be of much interest to know, which of these radicals participate in the follow-up electron transfers.

To get a closer insight we computed oxidation potentials of radicals **46a•**–**46d•**. To our surprise, **46a•** has still a high oxidation potential around 1.75 V_{SCE}, even though it is shifted ~1000 mV cathodically compared to that of a prototypical α,α-dicarbonyl alkyl radical (2.72 V_{SCE} for cyclohexanedione radical).[1a] Radical **46c•** (1.26 V_{SCE}) was found to be ~500 mV cathodically shifted in comparison to **46a•**, with its oxidation potential being similar to that of α-carbonyl radicals with one α-electron-withdrawing group. The oxidation potential of radical **46b•** (1.37 V_{SCE}) is similar to that of **46c•** in line with our expectations. The 110 mV anodic shift of the oxidation potential could be due to the fact that in **46c•** the α-carbonyl radical is of a ketone type while in **46b•** it is of the ester type. Most likely, **46c•** is the strongest reducing agent in acetonitrile. Of different range is the oxidation potential of radical **46d•**, which was calculated to be 0.20 V_{SCE} in acetonitrile but requires water to form. The oxidation potential of **46d•** is similar to that of an α-hydroxyalkyl radical,[54] as reported by Wayner et al.,[55] all of them placed in the range of −0.61 V_{SCE} to +0.38 V_{SCE} depending on the substituents. It was also noted that the oxidation potentials of α-hydroxyalkyl radicals are strongly dependent on the solvent used and are significantly lower in water than those obtained in acetonitrile.[56] The main reason for this large solvent effect was attributed to the better ion solvation properties of water compared to that of acetonitrile. In water, not only the reducing power of **46a•**–**46c•** is distinctly stronger, but deprotonation reactions are possible due to the higher basicity of the solvent. Thus, radicals **46a•**–**46c•** may afford the dehydroascorbate radical anion **46a**$^{-\bullet}$ by deprotonation and dehydration. The latter species is such a strong reductant that it should become the dominant secondary reducing species in water.

4. Conclusion

An extensive electrochemical investigation on 40 model enols was carried out by cyclic voltammetry showing a range of E_{pa} from 0.13 to 0.95 V_{Fc}. A few of the resulting enol radical cations were characterized by spectroscopic means (EPR, ENDOR). For the first time, oxidation potentials of enols derived from amides were reported. Their high E_{pa} potentials suggest that the two additional electron-withdrawing groups play an important role in the oxidation. Electronically seen, these systems are not only enols, but equally enamines.

The oxidation potentials of the enolates proved to be lower than those of the enols by about 1.1–1.6 V, which allowed an easy access to α-carbonyl radicals by oxidation of the enolates. The radicals were characterized by various techniques, such as EPR, ENDOR, magnetic susceptibility and cyclic voltammetry.

A different reactivity under oxidative conditions was observed for α-carbonyl radicals derived from enols with β-electron-withdrawing groups as compared those with β-electron-donating groups. While α-carbonyl radicals derived from the latter type of enols, e.g. β,β-dimesityl enols, are easily oxidized and undergo reactions typical of carbocations, α-carbonyl radicals derived from enols with β-electron-withdrawing groups will typically undergo radical follow-up reactions.

Using stable and hindered enols, it was possible to measure the oxidation potentials of a wide range of α-carbonyl radicals. A correlation was obtained, when AM1 calculated ionization potentials corrected for the solvation term were plotted against the experimentally determined oxidation potentials of α-carbonyl radicals. The correlation was useful in predicting the oxidation potential of the α-carbonyl radical derived from a simple thioester, a mimic for the enzyme substrate in dehydrogenases, suggesting that while the first electron transfer between the riboflavin derivatives FAD or FMN is possible, the second electron transfer would be very difficult. Rather, the radical intermediate will undergo a hydrogen atom transfer or a radical addition to the cofactor under enzyme conditions.

The correlation was also used to compute oxidation potentials of various ascorbic acid radicals formed after one-electron transfer or addition of hydroxyl radical to ascorbic acid. It was found that **46c**• had the lowest oxidation potentials of all possible neutral radicals in acetonitrile. Considering all species, however, it is the ascorbate radical anion, which has the lowest oxidation potential and thus is the strongest reducing agent.

In brief, oxidation potentials of enolates, α-carbonyl radicals and enols can provide valuable insight into their role as intermediates in preparative and enzymatic processes.

5. Experimental

5.1. Cyclic voltammetry

All CV measurements were carried out with a three-electrode system with 1 mm platinum disc electrode as working electrode, a Pt wire counter electrode and a Ag reference electrode all being placed into the solution. The cyclic voltammograms were recorded at various scan rates using a manifold of starting and reversal potentials. For determination of the oxidation potentials, ferrocene or triphenylpyrylium tetrafluoroborate or decamethylferrocene was added as internal standard. Tetra-*n*-butylammonium hexafluorophosphate was used as electrolyte. For fast scan cyclic voltammetry investigations, 385 mg (1.00 mmol) of supporting electrolyte, 50 μmol of substrate and 4.0 mL of solvent were used. Fast scan cyclic voltammograms were carried out at 5, 10 and 25 μm Au ultramicro electrodes, with a Pt wire serving as counter electrode and a Ag wire as a pseudo-reference electrode. Standard CVs were recorded using a Princeton Applied Research Model 362 potentiostat with a Philips model PM 8271xYt-recorder for scan rates <1 V s^{-1}. For fast scan cyclic voltammetry, a Hewlett Packard (HP) Model 331A4 Function Generator was used, connected to a three-electrode potentiostat developed by Amatore et al.[57] Data were recorded by an HP 54510 A digitizing oscilloscope linked to a 486DX33 computer using the HP data transfer program Scopelink. For generating enolates (under preparative as well as for cyclic voltammetry) tetramethylammonium hydroxide (25% solution in methanol) was used as base.

5.2. Computations

For the correlation in Figure 8, radicals (see Chart 2) with known oxidation potentials were computed by AM1 (Spartan). The corresponding cation was also optimized at the same level of computation (Table 8). The adiabatic ionization potential (IP_a^{gas}) was obtained by subtracting the heats of formation (ΔH_f) of the cation (C) from that of the radical (**R**•). The adiabatic ionization potential was corrected for the solvation term ($IP_a^{gas} - \Delta E_{solv}^{ACN}$). The solvation term ($\Delta E_{solv}^{ACN}$) was obtained from the Born equation (Table 9):

$$\Delta E_{solv}^{ACN} = \frac{-N_L Z^2 e^2}{2r}\left[1 - \frac{1}{\varepsilon}\right] \quad (4)$$

Details to Eq. 4: ε is the dielectric constant of the solvent; ACN=acetonitrile; r is the ionic radius of the carbocation, which was obtained from the surface area of the carbocation; N_L is the Avogadro's number and e is the charge of an electron.

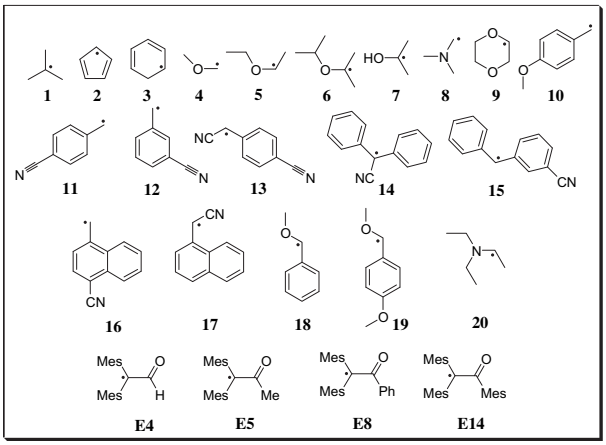

Chart 2. List of radicals used in Figure 8 for the correlation of IP_a^{gas} with the experimentally determined oxidation potential.

5.3. DFT computations

For the calculations of the isotropic hyperfine coupling constants the UB3LYP/6-31G* level of theory was applied using the Gaussian 94 program suite.[58]

Table 8
Calculation of gas phase adiabatic ionization potential of various radicals and their corresponding cations using the semiempirical method (AM1, Spartan)

Radical	Radical (R) ΔH_f/kcal mol^{-1}	Cation (C) ΔH_f/kcal mol^{-1}	IP_a^{gas} (C−R)/ kcal mol^{-1}	IP_a^{gas}/eV
1	−6.1	174.8	180.9	7.85
2	61.9	269.2	207.3	8.99
3	28.8	206.0	177.2	7.68
4	−22.8	158.0	180.8	7.84
5	−38.2	131.0	169.2	7.34
6	−49.2	111.6	160.8	6.97
7	−46.2	125.5	171.7	7.45
8	21.6	174.7	153.1	6.64
9	−67.3	109.1	176.4	7.65
10	0.0	173.2	173.2	7.51
11	69.6	262.3	192.7	8.36
12	70.0	262.0	192	8.33
13	98.2	300.7	202.5	8.78
14	97.9	281.6	183.7	7.97
15	89.7	270.3	180.6	7.83
16	86.1	274.0	187.9	8.15
17	82.3	270.6	188.3	8.17
18	−5.9	161.9	167.8	7.28
19	−44.3	117.3	161.6	7.01
28	0.3	146.2	145.9	6.33
R4•	−2.8	173.1	175.9	7.63
R5•	−8.0	165.8	173.8	7.54
R8•	27.3	200.0	172.7	7.45
R14•	13.8	183.8	170	7.37

Table 9
Solvent corrected adiabatic ionization potential of various radicals used in Figure 8 using the surface area method for incorporating the radius in the Born equation. The last column represents the experimentally determined oxidation potential of the corresponding radicals in acetonitrile, determined either by Wayner et al.[36] or in the present work

Radical	Surface area/Å^2	Radius r/Å	ΔE_{solv}^{ACN}/ kcal mol^{-1}	ΔE_{solv}^{ACN}/eV	$(IP_a^{gas}-\Delta E_{solv}^{ACN})$/eV	$E_{1/2}^{ox}$/ V_{SCE}
1	110.5	2.97	53.58	2.32	5.52	0.09
2	103.6	2.87	55.45	2.402	6.59	0.80
3	118.5	3.07	51.84	2.25	5.44	-0.04
4	82.8	2.57	61.92	2.69	5.16	−0.24
5	124.2	3.14	50.68	2.20	5.14	−0.45
6	160.3	3.57	44.586	1.93	5.04	−0.10
7	99.9	2.827	56.29	2.445	5.01	−0.60
8	107.3	2.921	54.48	2.36	4.28	−1.03
9	113.0	3.00	53.04	2.30	5.35	−0.08
10	163.3	3.60	44.20	1.921	5.59	0.51
11	154.0	3.50	45.47	1.97	6.39	1.03
12	154.0	3.50	45.47	1.97	6.36	1.11
13	173.5	3.728	42.69	1.85	6.93	1.63
14	224.9	4.23	37.62	1.63	6.34	1.01
15	231.4	4.29	37.09	1.61	6.22	0.56
16	196.3	3.95	40.29	1.75	6.40	0.72
17	196.9	3.96	40.19	1.74	6.42	0.97
18	165.1	3.62	43.96	1.91	5.37	−0.44
19	195.0	3.94	40.39	1.75	5.26	−0.55
28	163.4	3.61	44.08	1.91	4.42	−1.12
R4$^{\bullet}$	325.4	5.09	31.26	1.36	6.27	0.76
R5$^{\bullet}$	342.2	5.23	30.43	1.32	6.22	0.59
R8$^{\bullet}$	396.8	5.62	28.32	1.23	6.26	0.63
R14$^{\bullet}$	438.4	5.91	26.93	1.17	6.20	0.66

5.4. EPR, ENDOR, and general TRIPLE

EPR spectra were taken on a Varian E9 spectrometer whereas the ENDOR and general TRIPLE measurements were performed on a Bruker ESP300 instrument. All instruments were equipped with variable temperature units. EPR simulations were performed with the public domain program WinSim.

6. Synthesis

6.1. *Z*-2-Mesityl-2-(*p*-tolyl)ethenol (E2)[59]

In an inert atmosphere lithium aluminum hydride (700 mg, 18.4 mmol) was added to mesityl-*p*-tolyl ketene (2.20 g, 8.86 mmol) in anhydrous THF (40 mL). Stirring in an ice bath was continued until gas evolution stopped. Then the reaction mixture was stirred for 1 h at room temperature and stirred for additional 2 h at 80 °C. After cooling the solution was hydrolyzed with water (10 mL). After drying ($MgSO_4$) the solvent was removed in vacuo. The crude product was chromatographed under medium pressure (medium pressure liquid chromatography) with *n*-hexane/dichloromethane (1:2) as the eluent. Yield: 390 mg (17%). Mp 86–86.5 °C. Purity by GC (OV17, 25 m): 99%. IR (CCl_4): 3480 (vs, OH), 2900 (s, C–H), 1610 (vs, C=C), 1590 (m, C=C), 1420 (w), 1365 (w), 1290 (w), 1180 (m), 1130 (vs), 1060 (vs), 870 (w). ^{1}H NMR (250 MHz, $CDCl_3$): δ 2.10 (s, 6H, *o*-Mes–CH_3), 2.28 (s, 3H, *p*-Mes–CH_3), 2.32 (s, 3H, *p*-Tol–CH_3), 4.26 (d, J=14 Hz, OH), 6.95 (s, 2H, Mes–H), 6.95 (d, J=14 Hz, 1-H), 7.00 (m_{AB}, 4H, Tol–H). ^{13}C NMR ($CDCl_3$, 63 MHz): δ 19.8, 21.1, 21.2, 116.9, 124.5, 128.4, 129.0, 129.4, 130.0, 135.0, 135.5, 138.4, 138.5. HRMS (70 eV): calcd 252.1512, found 252.1510.

6.2. Z-2-(*p*-Anisyl)-2-mesitylethenol (E3)[22]

In an inert atmosphere, 1-mesityl-2-(4-methoxyphenyl)-ethylene glycol (3.00 g, 10.4 mmol), glacial acetic acid (30 mL) and concentrated hydrochloric acid (8 mL) were refluxed for 1 h. After cooling the reaction mixture was hydrolyzed with water (300 mL) and the crude product (2.23 g, 8.31 mmol, 80%) precipitated. The crude product consisted of the desired enol **E3** and its tautomeric aldehyde (55:45, as determined by GC on an SE30, 25 m). Separation of the tautomers failed due to the rapid tautomerization rate. ^{1}H NMR (250 MHz, $CDCl_3$): δ 2.10 (s, 6H, *o*-Mes–CH_3), 2.31 (s, 3H, *p*-Mes–CH_3), 3.79 (s, 3H, CH_3O), 5.04 (s, 1H, OH), 6.60–7.00 (m, 7H, Ar–H, C*H*OH).

6.3. 1,1-Dimesityl-1-hexen-2-ol (E6)

To a solution of dimesitylketene (1.50 g, 5.39 mmol) in dry ether (30 mL), kept at 0 °C in an inert atmosphere, 1.4 M *n*-butyllithium in hexane (3.9 mL, 5.50 mmol) was added dropwise. The mixture was stirred for additional 1.5 h at 0 °C and 1 h at room temperature. After the mixture had been hydrolyzed by adding half-saturated aq NH_4Cl solution (10 mL), the aqueous layer was extracted with diethyl ether (3×15 mL). The combined organic layers were dried and the solvent was removed in vacuo. The remaining brown oil was chromatographed twice on silica gel using cyclohexane/ethyl acetate (1:1) and cyclohexane/DCM (2:1) as eluent. Yield: 789 mg (43%). IR (neat): 3524 (s, OH), 3474 (s, OH), 2926 (s, C–H), 1626 (s), 1450 (s), 1375 (m), 1227 (m), 1176 (m), 851 (m) cm^{-1}. ^{1}H NMR (200 MHz, $CDCl_3$): δ 0.83 (t, J=7 Hz, 3H, 6-CH_3), 1.29 (m, 2H, 5-CH_2), 1.56 (m, 2H, 4-CH_2), 2.15 (m, 14H, *o*-Mes–CH_3+3-CH_2), 2.37 (s, 6H, *p*-Mes–CH_3), 4.93 (s, 1H, OH), 6.80 (s, 2H, Mes–H), 6.85 (s, 2H, Mes–H). ^{13}C NMR ($CDCl_3$, 63 MHz): δ 13.9, 18.4, 20.8, 20.9, 21.0, 22.8, 29.3, 31.2, 109.1, 129.0, 129.9, 132.3, 135.2, 135.3, 136.5, 138.4, 139.0, 152.4. HRMS (70 eV): calcd 336.2453, found 336.2454.

6.4. 1-(4-Bromophenyl)-2,2-dimesitylethenol (E9)

In an inert atmosphere, a solution of 2.45 M *n*-butyllithium in hexane (2.60 mL, 6.36 mmol) was added quickly to an ice-cooled solution of 1,4-dibromobenzene (1.50 g, 6.36 mmol) in dry ether (30 mL). A solution of dimesitylketene (1.67 g, 6.00 mmol) in dry ether (30 mL) was added after 1 min. Stirring was continued for 3 h at 0 °C and for an additional hour at room temperature. The mixture was hydrolyzed with half-saturated NH_4Cl solution (50 mL), washed with ether (3×30 mL), and evaporated after drying the organic layer ($MgSO_4$). Chromatography of the remaining oil on silica gel using cyclohexane/ethyl acetate (3:1) as the eluent and crystallization from ethanol yielded the pure **E9**. Yield: 1.11 g (40%). Mp 161–163 °C. IR (KBr): 3506 (s, OH), 2916 (s, C–H), 1610 (s, C=C), 1484, 1214, 1060, 1009, 849, 835, 741 cm^{-1}. ^{1}H NMR (250 MHz, $CDCl_3$): δ 1.90 (s, 3H, Mes–CH_3), 2.20 (s, 3H, Mes–CH_3), 2.27 (s, 12H, Mes–CH_3), 5.15 (s, 1H, OH), 6.68 (s, 2H, Mes–H), 6.89 (s, 2H, Mes–H), 7.18 (d, 2H, J=9 Hz, Ar–H), 7.28 (d, 2H, J=9 Hz, Ar–H). ^{13}C NMR ($CDCl_3$, 63 MHz): δ 20.6, 20.8, 21.2, 112.2, 122.2, 129.4, 129.9, 130.2, 130.8, 132.5, 134.9, 135.3, 136.1, 137.0, 137.9, 139.0, 149.3. Elemental analysis for $C_{26}H_{27}BrO$: calcd C 71.72%, H 6.25%; found C 71.62%, H 5.97%.

6.5. 1-(5-Bromo-2-methoxyphenyl)-2,2-dimesitylethenol (E12)

To a solution of 2.3 M *n*-butyllithium (5.52 mL, 12.7 mmol) in dry diethyl ether (70 mL) kept at −20 °C was added a solution of 4-bromo-1-methoxybenzene (2.40 g, 12.7 mmol) in dry ether (18 mL) under an argon blanket. After stirring for 30 min at this temperature a solution of dimesitylketene (3.52 g, 12.7 mmol) in dry ether (20 mL) was added and stirring continued for an additional 90 min at −18 °C. Then, while stirring, the temperature was slowly raised to room temperature over 60 min and kept for 120 min. The reaction mixture was poured in ice water (200 mL) and acidified with concd HCl (1 mL) and 2 N HCl (20 mL). The aqueous layer was extracted with diethyl ether (200 mL) and the

combined organic layers were extracted with concd NH_4Cl solution, dried ($MgSO_4$) and evaporated. The residue was chromatographed on silica gel to separate off the dimesitylacetic acid. A second chromatography on silica gel (0.060–0.200 μm) under medium pressure (flow 10 mL min^{-1}, 10 bar) with cyclohexane/DCM (1:2) as eluent yielded enols **E11** and **E12**.[60] Pure **E12** (301 mg, 13%) was obtained after crystallization from petroleum ether. Mp 201–201.5 °C. IR (CCl_4) 3500 (vs), 3000, 2910, 2830, 1600 (vs), 1590, 1440, 1270, 1210, 1180, 1060, 1030, 850 cm^{-1}. ^1H NMR (400 MHz, $CDCl_3$) δ 1.60–2.70 ([including signals at 1.90 (s, 6H), 2.14 (s, 3H), 2.27 (s, 3H)], total 18H, coalescence, Mes–CH_3), 3.47 (s, 3H, CH_3O), 5.32 (s, 1H, OH), 6.60 (d, *J*=9.9 Hz, 1H, *m*-aryl–H), 6.61 (s, 2H, Mes–H), 6.82 (s, 2H, Mes–H), 7.25 (dd, *J*=9.9 and 1.0 Hz, 1H, *p*-aryl–H), 7.37 (d, 1H, *J*=1.0 Hz, *o*-aryl–H). ^{13}C NMR ($CDCl_3$, 100 MHz): δ 20.8, 20.9, 21.2, 55.3, 112.2, 112.9, 115.2, 127.9, 128.9, 129.0, 129.8, 132.2, 133.0, 134.5, 135.2, 135.5, 136.7, 139.0, 146.1, 156.3. MS (70 eV): *m*/*z* (%)=467 (29), 466 (100), 465 (30), 464 (98). HRMS (70 eV) of $C_{27}H_{29}{}^{79}BrO_2$: calcd 464.1351, found 464.1370.

6.6. 1,1-Dimesityl-5-(triisopropylsilyloxy)pent-1-en-3-yn-2-ol (E29)

Triisopropylsilyloxy-2-propyne (1.07 g, 5.04 mmol) was added to ethylmagnesium bromide, generated from ethyl bromide (0.600 g, 5.50 mmol) and magnesium (0.133 g, 5.50 mmol) in 10 mL THF (dry), at room temperature. After the effervescence of hydrogen gas had stopped, 15 mL of a solution of dimesitylketene in THF (1.31 g, 4.71 mmol) was added. The reaction mixture was stirred at room temperature for 12 h and quenched with water. The reaction mixture was extracted with dichloromethane (2×25 mL), dried over Na_2SO_4 (anhyd) and concentrated yielding a colorless solid. It was recrystallized from hot pentane. Yield: 0.900 g (39%), mp 98–99 °C, IR (NaCl): 3269 (br s, OH), 2919, 2864 (alkyl), 2214 (alkyne), 1612 (C=C), 1463, 1368, 1247, 1138, 1062 (aromatic), 1015, 882, 852, 725, 689, 584 cm^{-1}. ^1H NMR ($CDCl_3$, 200 MHz): δ 0.98 (s, 21H, 7-H), 2.12–2.25 (br s, coalescence, 18H, 8-H), 4.43 (s, 2H, 1-H), 4.71 (br s, 1H, OH), 6.77 (br s, coalescence, 2H, 11-H), 6.86 (br s, coalescence, 2H, 13-H). ^{13}C NMR ($CDCl_3$, 50 MHz): δ 12.9 (C-6), 18.9 (C-7), 21.8 (C-8a), 22.2 (C-8b), 53.3 (C-1), 81.6 (C-2), 91.6 (C-3), 122.2 (C-4), 130.0 (C-5), 130.1, 130.7, 132.3, 134.6, 135.1, 137.0, 138.3, 139.4. Elemental analysis for $C_{32}H_{46}O_2Si$ (490.79): calcd C 78.31%, H 9.45%; found C 78.16%, H 9.70%.

6.7. 1,1-Dimesityl-6-(triisopropylsilyloxy)hex-1-en-3-yn-2-ol (E30)

Triisopropylsilyoxy-3-butyne (2.0 g, 8.8 mmol) was added to ethylmagnesium bromide, generated from ethyl bromide (1.1 g, 10 mmol) and magnesium (0.24 g, 10 mmol) in 20 mL of dry THF at room temperature. After the effervescence of hydrogen gas had stopped, 25 mL of a solution of dimesitylketene (2.5 g, 9.0 mmol) in THF was added. The reaction mixture was stirred at room temperature for 12 h and quenched with water. The reaction mixture was extracted with dichloromethane (2×25 mL), dried over Na_2SO_4 (anhyd) and concentrated yielding a colorless crystalline solid, which was recrystallized from hot pentane. Yield: 1.4 g (31%). Mp 126–128 °C. IR (NaCl): 3273 (br s, OH), 2956, 2916, 2863 (alkyl), 2727, 2214 (alkyne), 1721, 1610 (C=C), 1561, 1474, 1370, 1241, 1137, 1060 (aromatic), 1015, 965, 902, 885, 851, 828, 764, 696, 641, 567, 506 cm^{-1}. ^1H NMR ($CDCl_3$, 200 MHz): δ 1.04 (s, 21H, 7 and 8-H), 2.12–2.25 (br s, coalescence, 18H, 9a and 9b-H), 2.49 (t, *J*=7 Hz, 2H, 2-H), 3.68 (t, *J*=7 Hz, 2H, 1-H), 4.73 (br s, 1H, OH), 6.76 (br s, coalescence, 2H, 12-H), 6.86 (br s, coalescence, 2H, 14-H). ^{13}C NMR ($CDCl_3$, 50 MHz): δ 12.9, 18.9, 21.8, 22.3, 24.9, 62.6, 91.1, 120.0, 129.9, 130.0, 130.7, 132.5, 135.0, 135.5, 136.9, 138.1, 138.3, 139.4.

6.8. 1,1-Dimesityl-7-(triisopropylsilyloxy)hept-1-en-3-yn-2-ol (E31)

Triisopropylsilyloxy-4-pentyne (2.0 g, 8.3 mmol) was added to ethylmagnesium bromide, generated from ethyl bromide (1.0 g, 9.2 mmol) and magnesium (0.20 g, 8.3 mmol) in 20 mL of dry THF at room temperature. After the effervescence of hydrogen gas had stopped, 25 mL of a solution of dimesitylketene (2.5 g, 9.0 mmol) in THF was added. The reaction mixture was stirred at room temperature for 12 h and quenched with water. The reaction mixture was extracted with dichloromethane (2×25 mL), dried over Na_2SO_4 (anhyd) and concentrated affording a brown oil. Yield: 3.73 g (86%). ^1H NMR ($CDCl_3$, 200 MHz): δ (ppm): 1.03 (s, 21H, 8 and 9-H), 1.64 (q, *J*=6 Hz, 2H, 2-H) 1.99–2.28 (br s, coalescence, 18H, 10a and 10b-H), 2.38 (t, *J*=7 Hz, 2H, 3-H), 3.53 (t, *J*=6 Hz, 2H, 1-H), 4.72 (br s, 1H, OH), 6.77 (br s, coalescence, 2H, 14-H), 6.86 (br s, coalescence, 2H, 15-H). ^{13}C NMR ($CDCl_3$, 50 MHz): δ (ppm) 12.9, 16.8, 19.0, 21.8, 21.9, 32.4, 62.4, 94.2, 120.5, 129.9, 130.0, 130.7, 132.6, 135.1, 135.7, 136.8, 138.1, 139.5.

6.9. 5,5-Dimesitylpent-4-en-2-yne-1,4-diol (E32)

1,1-Dimesityl-5-(triisopropylsilyloxy)pent-1-en-3-yn-2-ol (0.40 g, 0.82 mmol) was added to a solution of aqueous acidic methanol, prepared by dissolving 5 mL of 10% sulfuric acid in 15 mL of methanol. The reaction mixture was stirred for 12–14 h and monitored by TLC. After the complete consumption of starting material, the reaction mixture was quenched with solid $NaHCO_3$ and concentrated. The residue was extracted with dichloromethane (2×25 mL), dried over Na_2SO_4 (anhyd) and concentrated. The crude product was purified by column chromatography with 60: 40 ether/hexane mixture as eluent (R_f=0.5). Yield: 0.23 g (84%). Mp 154–155 °C. IR (NaCl): 3413 (s, OH, non-hydrogen bonded), 3197 (br s, OH, hydrogen bonded), 2957, 2919, 2857 (alkyl), 2219 (alkyne), 1610 (C=C), 1474, 1445, 1375, 1262, 1203, 1178, 1097, 1046, 998, 967, 900, 856, 805, 594. ^1H NMR ($CDCl_3$, 200 MHz): δ 1.60 (br s, 1H, OH), 2.17–2.24 (br s, coalescence, 18H, 6a and 6b-H), 4.28 (s, 2H, 1-H), 4.85 (s, 1H, OH), 6.80 (br s, coalescence, 2H, 9-H), 6.86 (br s, coalescence, 2H, 10-H). ^{13}C NMR ($CDCl_3$, 50 MHz): δ 21.8, 22.2, 52.4, 82.8, 90.9, 122.5, 130.0, 130.2, 130.8, 132.0, 134.6, 134.8, 137.4, 138.5, 139.4. Elemental analysis for $C_{23}H_{26}O_2$ (334.45): calcd C 82.60%, H 7.84%, found C 82.25%, H 8.09%.

6.10. 6,6-Dimesitylhex-5-en-3-yn-1,5-diol (E33)

1,1-Dimesityl-6-(triisopropylsilyloxy)hex-1-en-3-yn-2-ol (0.60 g, 1.2 mmol) was added to a 20 mL solution of aqueous acidic methanol, prepared by dissolving 5 mL of 10% sulfuric acid to 15 mL of methanol. The reaction mixture was stirred for 12–14 h, while monitoring it by TLC. After complete consumption of the starting material the reaction mixture was quenched with solid $NaHCO_3$. The concentrated residue was extracted with dichloromethane (2×25 mL), and dried over Na_2SO_4 (anhyd). The crude product was purified by column chromatography with ether/hexane 60:40 as eluent (R_f=0.5). Yield: 325 mg (78%). Mp 192–194 °C. IR (film): 3430 (s, OH, non-hydrogen bonded), 3173 (br s, OH, hydrogen bonded), 3017, 2995, 2958, 2916 (alkyl), 2853, 2214 (alkyne), 1611 (C=C), 1475, 1439, 1373, 1355, 1289, 1238, 1165, 1138, 1035, 902, 849, 821, 735, 683, 582 cm^{-1}. ^1H NMR ($CDCl_3$, 200 MHz): δ 1.6 (br s, 1H, OH), 2.17–2.24 (br s, coalescence, 18H, 7a and 7b-H), 2.49 (t, *J*=6 Hz, 2H, 2-H), 3.57 (t, *J*=6 Hz, 2H, 1-H), 4.88 (br s, 1H, OH), 6.82 (br s, coalescence, 2H, 10-H), 6.86, (br s, coalescence, 2H, 12-H). ^{13}C NMR ($CDCl_3$, 50 MHz): δ 21.8, 25.0, 36.9, 61.7, 90.8, 121.4, 130.9, 132.1, 135.3, 135.4, 137.9, 138.3, 139.4, 139.6. HRMS for $C_{24}H_{28}O_2$: calcd 348.2089, found 348.2093.

6.11. 7,7-Dimesitylhept-6-en-4-yne-1,6-diol (E34)

1,1-Dimesityl-7-(triisopropylsilyloxy)hept-1-en-3-yn-2-ol (2.0 g, 3.9 mmol) was added to a solution of aqueous acidic methanol, prepared by dissolving 5 mL of 10% sulfuric acid to 15 mL of methanol. The reaction mixture was stirred for 12–14 h while monitoring it by TLC. After complete consumption of the starting material the reaction mixture was quenched with solid $NaHCO_3$. The residue was extracted with dichloromethane (2×25 mL) and dried over Na_2SO_4 (anhyd). The crude product was purified by column chromatography with DCM/ether 90:10 (R_f=0.7). Yield: 1.2 g (86%). Mp 141–142 °C. IR (film): 3435 (s, OH, non-hydrogen bonded), 2952, 2223 (alkyne), 1609 (C=C), 1474, 1454, 1350, 1239, 1193, 1137, 1054, 1032, 993, 899, 849, 819, 733, 564 cm^{-1}. ^1H NMR ($CDCl_3$, 200 MHz): δ 1.21 (br s, 1H, OH), 1.63 (q, J=6 Hz, 2H, 2-H) 2.12–2.25 (br s, coalescence, 18H, 8a-H and 8b-H), 2.36 (t, J=6 Hz, 2H, 3-H), 3.45 (t, J=6 Hz, 2H, 1-H), 4.84 (br s, 1H, OH), 6.80 (br s, coalescence, 2H, 12-H), 6.86 (br s, coalescence, 2H, 13-H). ^{13}C NMR ($CDCl_3$, 50 MHz): δ 21.9, 22.1, 31.5, 62.2, 78.3, 93.4, 120.8, 129.8, 130.7, 132.4, 135.3, 135.7, 137.0, 138.2, 139.4. Elemental analysis for $C_{25}H_{30}O_2$ (362.5): calcd C 82.83%, H 8.34%, found C 82.30%, H 8.66%.

6.12. 2-(*n*-Butyl)-3-mesityl-4,6,7-trimethylbenzofuran (B6)

Two test tubes were loaded with enol **E6** (572 mg, 169 μmol) and $[Fe(phen)_3](PF_6)_3$ (349 mg, 338 μmol), then to each CH_3CN (3.0 mL) was added by syringe. The oxidant solution was added to the enol solution. After 1 min the reaction was quenched with saturated $NaHCO_3$ solution (2.0 mL) and extracted with CH_2Cl_2 (2×15 mL). The combined organic layer was washed twice with saturated NaCl solution (2×10 mL) and dried over $MgSO_4$ (anhyd). The crude product was purified by chromatography on silica gel (cyclohexane/CH_2Cl_2 2:1) as yellow-greenish oil. Yield: 49.1 mg (86%). IR (neat): 2922 (s, C–H), 2861 (m), 1609 (m), 1455, 1377, 1094, 976, 851 (m). ^1H NMR (200 MHz, $CDCl_3$): δ 0.88 (t, J=7 Hz, 3H, 4″-CH_3), 1.35 (m, 2H, 3″-CH_3), 1.66 (m, 2H, 2″-CH_3), 1.85 (s, 3H, *p*-Mes–CH_3), 2.02 (s, 6H, *o*-Mes–CH_3), 2.34 (s, 6H, 4+6-Bf-CH_3), 2.43 (s, 3H, 7-Bf-CH_3), superimposed 2.47 (t, J=7 Hz, 3H, 1″-CH_3), 6.72 (s, 1H, 5-Bf–H), 6.93 (s, 2H, Mes–H). ^{13}C NMR ($CDCl_3$, 50 MHz): δ 11.4, 13.8, 17.1, 19.0, 20.5, 21.1, 26.4, 29.9, 114.7, 116.7, 124.8, 125.5, 127.5, 127.6, 130.1, 131.2, 136.8, 138.0, 153.4, 153.8. HRMS (70 eV) for $C_{24}H_{30}O$: calcd 334.2296, found: 334.2295.

6.13. 2-(4-Bromophenyl)-3-mesityl-4,6,7-trimethylbenzofuran (B9)

To a solution of enol **E9** (30.0 mg, 68.8 μmol) in acetonitrile (3.0 mL), a solution of $[Fe(phen)_3](PF_6)_3$ (142 mg, 138 μmol) was added under nitrogen. The reaction mixture was quenched with saturated $NaHCO_3$ (2.0 mL) and extracted with CH_2Cl_2 (2×15 mL). The combined organic layer was washed twice with saturated NaCl solution (2×10 mL), and dried over $MgSO_4$. The crude product was purified by chromatography on silica gel (cyclohexane/DCM 2:1). Yield: 28.7 mg (96%). ^1H NMR (200 MHz, $CDCl_3$): δ 1.86 (s, 3H, *p*-Mes–CH_3), 1.99 (s, 6H, *o*-Mes–CH_3), 2.37+2.38 (2s, 6H, 4- and 6-Bf–CH_3), 2.51 (s, 3H, 7-Bf–CH_3), 6.76 (s, 1H, 5-Bf–H), 6.97 (s, 2H, Mes–H), 7.37 (s, 4H, Ar–H). ^{13}C NMR ($CDCl_3$, 50 MHz): δ 11.5, 16.9, 19.1, 20.8, 21.3, 117.1, 121.4, 125.1, 125.4, 125.6, 127.1, 127.4, 127.7, 128.7, 129.2, 130.1, 130.5, 130.8, 132.5, 133.2, 137.2, 137.6, 146.9, 153.6. HRMS (70 eV): calcd 432.1089, found: 432.1093.

6.14. 2-(5-Bromo-2-methoxyphenyl)-3-mesityl-4,6,7-trimethylbenzofuran (B12)

To a solution of enol **E12** (13.4 mg, 28.8 μmol) in acetonitrile (10.0 mL), a solution of $[Fe(phen)_3](PF_6)_3$ (88.8 mg, 86.2 μmol) in acetonitrile was added. After 5 min, the reaction mixture was quenched with saturated $NaHCO_3$ solution (5.0 mL) and extracted with CH_2Cl_2 (2×10 mL). The combined organic layer was washed twice with saturated NaCl solution (2×10 mL) and dried over $NaSO_4$. The crude product was purified by column chromatography on silica gel (cyclohexane/CH_2Cl_2 2:1). Yield: 10.0 mg (75%). IR (CCl_4): 2915 (vs, C–H), 2850 (s), 1610 (m, C=C), 1590 (m, C=C), 1445 (s), 1250 (s), 1190 (m), 1120 (s), 1065 (s), 1040 (vs), 860 (w), 820 (m). ^1H NMR (250 MHz, $CDCl_3$): δ 1.88 (s, 3H, *p*-Mes–CH_3), 1.95 (s, 6H, *o*-Mes–CH_3), 2.29 (s, 3H, 4-Bf–CH_3), 2.37 (s, 3H, 6-Bf–CH_3), 2.44 (s, 3H, 7-Bf–CH_3), 3.45 (s, 3H, OCH_3), 6.68 (d, 1H, J=10 Hz, *m*-aryl–H), 6.75 (s, 1H, 5-Bf–H), 6.85 (s, 2H, Mes–H), 7.32 (dd, 1H, J=10, 4 Hz, *p*-aryl–H), 7.50 (d, 1H, J=4 Hz, *o*-aryl–H). ^{13}C NMR ($CDCl_3$, 100 MHz): δ 11.6, 17.3, 19.1, 20.6, 21.2, 55.3, 112.5, 113.3, 117.2, 118.9, 123.2, 125.1, 126.3, 127.8, 128.7, 130.5, 132.3, 133.0, 136.7, 137.5, 146.4, 154.4, 156.5. MS (70 eV): m/z (%)=465 (28), 464 (100), 463 (30), 462 (98). HRMS (70 eV) for $C_{27}H_{27}O_2{}^{79}Br$: calcd 462.1194, found: 462.1201.

Crystal structure determination of ***E29***: colorless crystals, size 1.60×0.90×0.70 mm^3. $C_{32}H_{46}O_2Si$ (M_r=490.8), triclinic, space group $P\bar{1}$ with a=8.407(2) Å, b=14.957(3) Å, c=25.124(5) Å, α=80.63(3)°, β=80.70(3)°, γ=74.22(3)°, V=2976.6(11) $Å^3$, Z=4, D_{calcd}=1.095 g cm^{-3}, λ=0.71073 Å. Intensity data were measured on an STOE-IPDS1 diffractometer. A total of 36,317 reflections were collected to a maximum 2θ value of 28.08° at 173(2) K; $-11\le h\le 11$, $-19\le k\le 19$, $-33\le l\le 33$. Data reduction and absorption correction from equivalents.[60] The structure was solved by direct methods[61] and refined by full-matrix least-squares on F^2. All non-hydrogen atoms were given anisotropic displacement parameters; hydrogen atoms were located from difference Fourier maps and refined at idealized positions riding on their parent atoms. The refinement converged at $R1$ ($I>2\sigma(I)$)=0.054, $wR2$ (all data)=0.1712 for 13,315 independent reflections and 660 variables. Min/max height in final ΔF-map −0.50/0.76 e $Å^{-3}$.

E29 (*aP*324) crystallizes triclinic in the space group P_1 with two formula units in the asymmetric unit. Intermolecular hydrogen bonds leading to dimers were observed in the solid state.

Table 10
Bond lengths, bond and dihedral angles in **E29** (two formula)

Bonds	d/pm[a]	d/pm[b]	Angles	Angle[a]/°	Angle[b]/°
C1=C2	135.2	134.6	C=C–O1	120.26	119.70
=C–O1	137.0	137.4	C–O1–H	109.47	109.47
C≡C	119.1	119.8	HOC=C	174.25	160.35
O1–H	82.0	82.0	O1C=CC6	−10.58	−9.33

[a] Eq. 1.
[b] Eq. 2.

Crystal structure determination of ***E34***: colorless crystals, size 0.40×0.35×0.35 mm^3. $C_{25}H_{30}O_2$ (M_r=362.5), triclinic, space group $P\bar{1}$ with a=8.0809(6) Å, b=9.7154(7) Å, c=14.4476(11) Å, α=82.184(2)°, β=81.136(1)°, γ=69.744(1)°, V=1047.2(1) $Å^3$, Z=2, D_{calcd}=1.150 g cm^{-3}, λ=0.71073 Å. Intensity data were measured on a Bruker-AXS SMART APEXCCD diffractometer. A total of 6148 reflections were collected to a maximum 2θ value of 26.4° at 150(2) K; h −8/+10, k −7/+12, l −18/+17. Data reduction and absorption correction from equivalents.[61] The structure was solved by direct methods[62] and refined by full-matrix least-squares[62] on F^2. All non-hydrogen atoms were given anisotropic displacement parameters; hydrogen atoms were located from difference Fourier maps and refined at idealized positions riding on their parent atoms. The refinement converged at $R1$ ($I>2\sigma(I)$)=0.043, $wR2$ (all data)=0.121 for 4168 independent reflections and 252 variables. Min/max height in final ΔF-map −0.18/0.22 e $Å^{-3}$.

Table 11
Bond lengths *d*, bond and dihedral angles in **E34**

Bonds	*d*/pm	Angles	Angle/°
C1═C2	134.7	C═C–O1	121.43
═C–O1	137.3	C–O1–H	109.42
C≡C	119.4	HOC═C	163.62
O1–H	84.0	OC═CC6	4.82

The crystallographic data (excluding structure factors) have been deposited with the Cambridge Crystallographic Data Centre as supplementary publication nos. CCDC 752574 (**E29**) and 752432 (**E34**). Copies of the data can be obtained, free of charge, on application to CCDC, 12 Union Road, Cambridge CB2 1EZ, UK (fax: +44 (0)1223 336033 or e-mail: deposit@ccdc.cam.ac.uk).

Acknowledgements

For generous financial support we are indebted to the DFG (priority program—Radicals in enzymatic catalysis), the BASF (fellowship to M.R.), the Volkswagen-Stiftung, the Fonds der Chemischen Industrie and University of Siegen. We thank Prof. Dr. J. P. Dinnocenzo (Rochester) for help with the magnetic susceptibility measurements.

Supplementary data

Supplementary data associated with this article can be found in online version at doi:10.1016/j.tet.2009.10.039.

References and notes

1. (a) Schmittel, M. *Top. Curr. Chem.* **1994**, *169*, 183–230; (b) Csákÿ, A. G.; Plumet, J. *Chem. Soc. Rev.* **2001**, *30*, 313–320; (c) Schmittel, M.; Haeuseler, A. *J. Organomet. Chem.* **2002**, *661*, 169–179; (d) Baran, P. S.; Ambhaikar, N. B.; Guerrero, C. A.; Hafensteiner, B. D.; Lin, D. W.; Richter, J. M. *ARKIVOC* **2006**, *vii*, 310–325.
2. (a) Kobayashi, Y.; Taguchi, T.; Morikawa, T. *Tetrahedron Lett.* **1978**, 3555–3556; (b) Paquette, L. A.; Snow, R. A.; Muthard, J. L.; Cynkowski, T. *J. Am. Chem. Soc.* **1978**, *100*, 1600–1602 and **1979**, *101*, 6991–6996; (c) Poupart, M.-A.; Lassalle, G.; Paquette, L. A. *Org. Synth.* **1990**, *69*, 173–179.
3. (a) Ito, Y.; Konoike, T.; Saegusa, T. *J. Am. Chem. Soc.* **1975**, *97*, 2912–2914; (b) Ito, Y.; Konoike, T.; Harada, T.; Saegusa, T. *J. Am. Chem. Soc.* **1977**, *99*, 1487–1493; (c) Frazier, R. H., Jr.; Harlow, R. L. *J. Org. Chem.* **1980**, *45*, 5408–5411; (d) Paquette, L. A.; Bzowej, E. I.; Branan, B. M.; Stanton, K. J. *J. Org. Chem.* **1995**, *60*, 7277–7283; (e) Jahn, U.; Müller, M.; Aussieker, S. *J. Am. Chem. Soc.* **2000**, *122*, 5212–5213; (f) Jahn, U.; Hartmann, P.; Dix, I.; Jones, P. G. *Eur. J. Org. Chem.* **2001**, 3333–3355; (g) Jahn, U.; Hartmann, P.; Dix, I.; Jones, P. G. *Eur. J. Org. Chem.* **2002**, 718–735; (h) Gevorkyan, A. A.; Arakelyan, A. S.; Barsegyan, S. V.; Petrosyan, K. A.; Panosyan, G. A. *Russ. J. Org. Chem.* **2003**, *39*, 1204–1205; (i) Jahn, U.; Hartmann, P.; Kaasalainen, E. *Org. Lett.* **2004**, *6*, 257–260; (j) Schmittel, M.; Lal, M.; Schlosser, M.; Deiseroth, H.-J. *Acta Crystallogr., Sect. C* **2004**, 589–591; (k) DeMartino, M. P.; Chen, K.; Baran, P. S. *J. Am. Chem. Soc.* **2008**, *130*, 11546–11560.
4. Cohen, T.; McNamara, K.; Kuzemko, M. A.; Ramig, K.; Landi, J. J., Jr.; Dong, Y. *Tetrahedron* **1993**, *49*, 7931–7942.
5. (a) Richter, J. M.; Whitefield, B. W.; Maimone, T. J.; Lin, D. W.; Castroviejo, M. P.; Baran, P. S. *J. Am. Chem. Soc.* **2007**, *129*, 12857–12869; (b) Li, Q.; Hurley, P.; Ding, H.; Roberts, A. G.; Akella, R.; Harran, P. G. *J. Org. Chem.* **2009**, *74*, 5909–5919.
6. Röck, M.; Schmittel, M. *J. Chem. Soc., Chem. Commun.* **1993**, 1739–1741.
7. (a) Schmittel, M.; Abufarag, A.; Luche, O.; Levis, M. *Angew. Chem., Int. Ed. Engl.* **1990**, *29*, 1144–1146; (b) Schmittel, M.; Levis, M. *Chem. Lett.* **1994**, 1935–1938; (c) Schulz, M.; Kluge, R.; Sivilai, L.; Kamm, B. *Tetrahedron* **1990**, *46*, 2371–2380.
8. (a) Schmittel, M.; Baumann, U. *Angew. Chem., Int. Ed. Engl.* **1990**, *29*, 541–543; (b) Schmittel, M.; Röck, M. *Chem. Ber.* **1992**, *125*, 1611–1620; (c) Röck, M.; Schmittel, M. *J. Prakt. Chem.* **1994**, *336*, 325–329; (d) Langels, M.; Langels, A. *J. Chem. Soc., Perkin Trans. 2* **1998**, 565–571; (e) Gebicki, J.; Marcinek, A.; Zielonka, J. *Acc. Chem. Res.* **2004**, *37*, 379–386.
9. Schepp, N. P. *J. Org. Chem.* **2004**, *69*, 4931–4935.
10. (a) Lai, M.; Liu, L.; Liu, H. *J. Am. Chem. Soc.* **1991**, *113*, 7388–7397; (b) Lenn, N. D.; Shih, Y.; Stankovich, M. T.; Liu, H. *J. Am. Chem. Soc.* **1989**, *111*, 3065–3067.
11. (a) Golding, B. T.; Radom, L. *J. Chem. Soc., Chem. Commun.* **1973**, 939–941; (b) Golding, B. T.; Radom, L. *J. Am. Chem. Soc.* **1976**, *98*, 6331–6338; (c) George, P.; Glusker, J. P.; Bock, C. W. *J. Am. Chem. Soc.* **1995**, *117*, 10131–10132.
12. Enol ethers: (a) Shono, T.; Matsumura, Y.; Hamaguchi, H.; Imanishi, T.; Yoshida, K. *Bull. Chem. Soc. Jpn.* **1978**, *51*, 2179–2180; (b) Koch, D.; Schäfer, H.; Steckhan, E. *Chem. Ber.* **1974**, *107*, 3640–3657; (c) Ogibin, Y. N.; Terent'ev, A. O.; Ilovaiskii, A. I.; Nikishin, G. I. *Russ. J. Electrochem.* **2000**, *36*, 193–202; (d) Okada, Y.; Akaba, R.; Chiba, K. *Org. Lett.* **2009**, *11*, 1033–1035; (e) Moeller, K. D. *Synlett* **2009**, 1208–1218.
13. Enol silanes: (a) Schmittel, M.; Keller, M.; Burghart, A. *J. Chem. Soc., Perkin Trans. 2* **1995**, 2327–2333; (b) Einaga, H.; Nojima, M.; Abe, M. *Main Group Met. Chem.* **1999**, *22*, 539–543; (c) Frey, D. A.; Reddy, S. H. K.; Moeller, K. D. *J. Org. Chem.* **1999**, *64*, 2805–2813; (d) Schmittel, M.; Burghart, A.; Malisch, W.; Reising, J.; Söllner, R. *J. Org. Chem.* **1998**, *63*, 396–400; (e) Schmittel, M.; Burghart, A.; Werner, H.; Laubender, M.; Söllner, R. *J. Org. Chem.* **1999**, *64*, 3077–3085; (f) Bunte, J. O.; Heilmann, E. K.; Hein, B.; Mattay, J. *Eur. J. Org. Chem.* **2004**, 3535–3550; (g) Sperry, J. B.; Whitehead, C. R.; Ghiviriga, I.; Walczak, R. M.; Wright, D. L. *J. Org. Chem.* **2004**, *69*, 3726–3734; (h) Uneyama, K.; Tanaka, H.; Kobayashi, S.; Shioyama, M.; Amii, H. *Org. Lett.* **2004**, *6*, 2733–2736; (i) Miller, A. K.; Hughes, C. C.; Kennedy-Smith, J. J.; Gradl, S. N.; Trauner, D. *J. Am. Chem. Soc.* **2006**, *128*, 17057–17062; (j) Clift, M. D.; Taylor, C. N.; Thomson, R. J. *Org. Lett.* **2007**, *9*, 4667–4669; (k) Jiao, J. L.; Zhang, Y.; Devery, J. J., III; xu, L.; Deng, J.; Flowers, R. A., II. *J. Org. Chem.* **2007**, *72*, 5486–5492; (l) Avetta, C. T.; Konkol, L. C.; Taylor, C. N.; Dugan, K. C.; Stern, C. L.; Thomson, R. J. *Org. Lett.* **2008**, *10*, 5621–5624.
14. Enol esters: (a) Shono, T.; Matsumura, Y.; Nakagawa, Y. *J. Am. Chem. Soc.* **1974**, *96*, 3532–3536; (b) Shono, T.; Okawa, M.; Nishiguchi, I. *J. Am. Chem. Soc.* **1975**, *97*, 6144–6147; (c) Schmittel, M.; Heinze, J.; Trenkle, H. *J. Org. Chem.* **1995**, *60*, 2726–2733; (d) Schmittel, M.; Steffen, J. P.; Burghart, A. *Acta Chem. Scand.* **1999**, *53*, 781–791; (e) Csákÿ, A. G.; Mula, M. B.; Mba, M.; Plumet, J. *Tetrahedron: Asymmetry* **2002**, *13*, 753–757; (f) Malkowsky, I. M.; Rommel, C. E.; Fröhlich, R.; Griesbach, U.; Pütter, H.; Waldvogel, S. R. *Chem.—Eur. J.* **2006**, *12*, 7482–7488.
15. (a) Bouma, W. J.; McLeod, J. K.; Radom, L. *J. Am. Chem. Soc.* **1979**, *101*, 5540–5545; (b) Holmes, J. L.; Lossing, J. P. *J. Am. Chem. Soc.* **1980**, *102*, 1591–1595 **1982**, *104*, 2648–2649; (c) Heinrich, N.; Koch, W.; Frenking, G.; Schwarz, H. *J. Am. Chem. Soc.* **1986**, *108*, 593–600; (d) Heinrich, N.; Louage, F.; Lifshitz, C.; Schwarz, H. *J. Am. Chem. Soc.* **1988**, *110*, 8183–8192; (e) Czerwinska, M.; Sikora, A.; Szajerski, P.; Adamus, J.; Marcinek, A.; Gebicki, J.; Bednarek, P. *J. Phys. Chem. A* **2006**, *110*, 7272–7278.
16. Fuson, R. C.; Rowland, S. P. *J. Am. Chem. Soc.* **1943**, *65*, 992–993.
17. (a) Nugiel, D. A.; Rappoport, Z. *J. Am. Chem. Soc.* **1985**, *107*, 3669–3676; (b) Nadler, E. B.; Rappoport, Z. *J. Am. Chem. Soc.* **1987**, *109*, 2112–2127; (c) Rappoport, Z.; Biali, S. E. *Acc. Chem. Res.* **1988**, *21*, 442–449.
18. Schmittel, M.; Langels, A. *Liebigs Ann.* **1996**, 999–1004.
19. Lal, M.; Langels, A.; Deiseroth, H.-J.; Schlirf, J.; Schmittel, M. *J. Phys. Org. Chem.* **2003**, *16*, 373–379.
20. Schmittel, M.; Lal, M.; Schenk, W. A.; Hagel, M.; Burzlaff, N.; Langels, A. *Z. Naturforsch., B* **2003**, *58b*, 877–884.
21. (a) Mukhopadhyaya, J. K.; Sklenák, S.; Rappoport, Z. *J. Am. Chem. Soc.* **2000**, *122*, 1325–1336; (b) Mukhopadhyaya, J. K.; Sklenák, S.; Rappoport, Z. *J. Org. Chem.* **2000**, *65*, 6856–6867; (c) Lei, Y. x.; Casarini, D.; Cerioni, G.; Rappoport, Z. *J. Org. Chem.* **2003**, *68*, 947–959; (d) Basheer, A.; Rappoport, Z. *J. Org. Chem.* **2004**, *69*, 1151–1160; (e) Basheer, A.; Yamataka, H,; Ammal, S. C.; Rappoport, Z. *J. Org. Chem.* **2007**, *72*, 5297–5312.
22. (a) Fuson, R. C.; Corse, J.; McKeever, C. H. *J. Am. Chem. Soc.* **1940**, *62*, 3250–3251; (b) Fuson, R. C.; Rabjohn, N.; Byers, D. J. *J. Am. Chem. Soc.* **1944**, *66*, 1272–1274.
23. (a) Hart, H.; Rappoport, Z.; Biali, S. E. In *The Chemistry of Enols*; Rappoport, Z., Ed.; Wiley: Chichester, UK, 1990; pp 481–589; (b) Hegarty, A. F.; O'Neill, P. In *The Chemistry of Enols*; Rappoport, Z., Ed.; Wiley: Chichester, UK, 1990; pp 639–650.
24. Nicholson, R. S.; Shain, I. *Anal. Chem.* **1964**, *36*, 706–723.
25. Schmittel, M.; Langels, A. *J. Org. Chem.* **1998**, *63*, 7328–7337.
26. Schmittel, M.; Gescheidt, G.; Röck, M. *Angew. Chem., Int. Ed. Engl.* **1994**, *33*, 1961–1963.
27. (a) Kern, J. M.; Federlin, P. *Tetrahedron Lett.* **1977**, 837–840; (b) Lochert, P.; Federlin, P. *Tetrahedron Lett.* **1973**, 1109–1112.
28. Evans, D. F. *J. Chem. Soc.* **1959**, 2003–2005.
29. Diêp Lê, K. H.; Lederer, F. *J. Biol. Chem.* **1991**, *226*, 20877–20881.
30. Walsh, C. *Acc. Chem. Res.* **1986**, *19*, 216–221.
31. Chesnut, D. B.; Sloan, G. J. *J. Chem. Phys.* **1961**, *352*, 443–444.
32. (a) Kubiak, B.; Lehnig, M.; Neumann, W. P.; Pentling, U.; Zarkadis, A. K. *J. Chem. Soc., Perkin Trans. 2* **1992**, 1443–1447; (b) Neumann, W. P.; Stapel, R. *Chem. Ber.* **1986**, *119*, 3422–3431.
33. (a) Oriac-Le Moing, M.-A.; Le Guillanton, G. *Electrochim. Acta* **1982**, *27*, 1775–1780; (b) Kern, J. M.; Sauer, J. D.; Federlin, P. *Tetrahedron* **1982**, *38*, 3023–3033.
34. Okamoto, K.; Takeuchi, K.; Kitagawa, T. *Bull. Soc. Chim. Belg.* **1982**, *91*, 410.
35. (a) Kitagawa, T.; Nishimura, M.; Takeuchi, K.; Okamoto, K. *Tetrahedron Lett.* **1991**, *32*, 3187–3190; (b) Biali, S. E.; Rappoport, Z. *J. Org. Chem.* **1986**, *51*, 964–970.
36. (a) Wayner, D. D. M.; Griller, D. *J. Am. Chem. Soc.* **1985**, *107*, 7764–7765; (b) Wayner, D. D. M.; McPhee, D. J.; Griller, D. *J. Am. Chem. Soc.* **1988**, *110*, 132–137; (c) Sim, B. A.; Milne, P. H.; Griller, D.; Wayner, D. D. M. *J. Am. Chem. Soc.* **1990**, *112*, 6635–6638; (d) Wayner, D. D. M.; Sim, B. A. *J. Org. Chem.* **1991**, *56*, 4853–4858; (e) Nagaoka, T.; Griller, D.; Wayner, D. D. M. *J. Phys. Chem.* **1991**, *95*, 6264–6270.
37. Orliac-Le Moing, M.-A.; Le Guillanton, G.; Simonet, J. *Electrochim. Acta* **1982**, *27*, 1775–1780.
38. Schmidt, D. M. Z.; Hubbard, B. K.; Gerlt, J. A. *Biochemistry* **2001**, *40*, 15707–15715.
39. Bohne, C.; MacDonald, D.; Dunford, H. B. *J. Am. Chem. Soc.* **1986**, *108*, 7867–7868.
40. Barnett, J. E.; Rasheed, A.; Corina, D. L. *Biochem. J.* **1973**, *131*, 21–30.

41. (a) Westheimer, F. *Proc. Chem. Soc.* **1963**, 253–261; (b) Leussing, D. L.; Emly, M. *J. Am. Chem. Soc.* **1984**, *106*, 443–444.
42. (a) Hill, R. L.; Teipel, J. W. In *The Enzymes*, 3rd ed.; Boyer, P., Ed.; Academic: New York, NY, 1971; Vol. V, pp 539–571; (b) Glusker, J. P. In *The Enzymes*, 3rd ed.; Boyer, P., Ed.; Academic: New York, NY, 1971; Vol. V, pp 413–439; (c) Arfin, S. M. *J. Biol. Chem.* **1969**, *244*, 2250–2251.
43. (a) Ghisla, S.; Thorpe, C.; Massey, V. *Biochemistry* **1984**, *23*, 3154–3161; (b) Fendrich, G.; Abeles, R. H. *Biochemistry* **1982**, *21*, 6685–6695.
44. Sonntag, C. *Free-Radical Induced DNA Damage and Its Repair—A Chemical Perspective*; Springer: Berlin, 2006.
45. Bennati, M.; Lendzian, F.; Schmittel, M.; Zipse, H. *Biol. Chem.* **2005**, *386*, 1007–1022.
46. Rizwan, A.; Armstrong, D. A. *Biochemistry* **1982**, *21*, 5445–5450.
47. James, T. H. *J. Am. Chem. Soc.* **1944**, *66*, 91–94.
48. David, N.; Michael, W.; Patric, M. K.; Brian, H. K.; Bernhard, H. S. *Biochemistry* **2001**, *40*, 11905–11911.
49. Franscisco, P.; Barry, A. C.; Richard, G. C. *J. Phys. Chem. B* **1998**, *102*, 7442–7447.
50. Sawyer, D. T.; Chiericato, G.; Tsuchiya, T. *J. Am. Chem. Soc.* **1982**, *104*, 6273–6278.
51. ÓMalley, P. J. *J. Phys. Chem. B* **2001**, *105*, 11290–11293.
52. Bielski, B. H. J.; Comstok, D. A.; Bowen, R. A. *J. Am. Chem. Soc.* **1971**, *93*, 5624–5629.
53. (a) Kirino, Y.; Kwan, T. *Chem. Pharm. Bull.* **1971**, *19*, 718–721; (b) Kirino, Y.; Kwan, T. *Chem. Pharm. Bull.* **1972**, *20*, 2651–2660; (c) Schöneshöfer, M. *Z. Naturforsch., Teil B* **1972**, *B27*, 649–659; (d) Laroff, G. P.; Fessenden, R. W.; Schuler, R. H. *J. Am. Chem. Soc.* **1972**, *94*, 9062–9073.
54. (a) Kolt, R. J.; Wayner, D. D. M.; Griller, D. *J. Org. Chem.* **1989**, *54*, 4259–4260; (b) Lilie, J.; Beck, G.; Henglein, A. *Ber. Bunsen-Ges. Phys. Chem.* **1971**, *75*, 458–465.
55. Lund, T.; Wayner, D. D. M.; Jonsson, M.; Larsen, A. G.; Daasbjerg, K. *J. Am. Chem. Soc.* **2001**, *123*, 12590–12595.
56. Wayner, D. D. M.; Houmam, A. *Acta Chem. Scand.* **1998**, *52*, 377–384.
57. Amatore, C.; Lefrou, C.; Pflüger, F. *J. Electroanal. Chem. Interfacial Electrochem.* **1989**, *270*, 42–59.
58. Frisch, M. J.; Trucks, G. W.; Schlegel, H. B.; Gill, P. M. W.; Johnson, B. G.; Robb, M. A.; Cheeseman, J. R.; Keith, T.; Petersson, G. A.; Montgomery, J. A.; Raghavachari, K.; Al-Laham, M. A.; Zakrzewski, V. G.; Ortiz, J. V.; Foresman, J. B.; Peng, C. Y.; Ayala, P. Y.; Chen, W.; Wong, M. W.; Andres, J. L.; Replogle, E. S.; Gomperts, R.; Martin, R. L.; Fox, D. J.; Binkley, J. S.; Defrees, D. J.; Baker, J.; Stewart, J. P.; Head-Gordon, M.; Gonzalez, C.; Pople, J. A. *Gaussian 94, Revision B.3*; Gaussian,: Pittsburgh, PA, 1995.
59. Fuson, R. C.; Maynert, E. W.; Tan, T.-L.; Trumbull, E. R.; Wassmundt, F. W. *J. Am. Chem. Soc.* **1957**, *79*, 1938–1941.
60. Enol **E11** has been described earlier, see Ref. 17b.
61. Sheldrick, G. M. *SADABS*; University of Göttingen: Göttingen, Germany, 2004.
62. Sheldrick, G. M. *Acta Crystallogr., Sect. A* **2008**, *64*, 112–122.